Annals of Glaciology

Glacier projections sensitivity to temperature-index model choices and calibration strategies

Journal:	*Annals of Glaciology*
Manuscript ID	AOG-90-0398
Manuscript Type:	Article
Date Submitted by the Author:	27-Feb-2023
Complete List of Authors:	Schuster, Lilian; Universität Innsbruck, Department of Atmospheric and Cryospheric Sciences (ACINN) Rounce, David; Carnegie Mellon University, Civil and Environmental Engineering Department Maussion, Fabien; Universität Innsbruck, Department of Atmospheric and Cryospheric Sciences (ACINN)
Keywords:	Mountain glaciers, Glaciological model experiments, Glacier volume, Glacier modelling, Glacier mass balance
Abstract:	Glacier models contribute significantly to the uncertainty of glacier change projections. In this study, we focus on temperature-index mass-balance (MB) models and their calibration, exploring the impact of various design choices on projections. Using the Open Global Glacier Model (OGGM), we compare the effects of different surface-type dependent degree-day factors, temporal climate resolutions (daily, monthly) and downscaling strategies (temperature lapse rates, temperature and precipitation correction) on projections for 88 glaciers

with in-situ observations. Our analysis shows that higher spatial and temporal resolution MB observations lead to more accurate MB gradient representations thanks to an improved calibration. Some choices have systematic effects. For example, weaker temperature lapse rates result in smaller glaciers in a warmer climate. However, we often find nonlinear effects, such as with the sensitivity to different degree-day factors for snow, firn, and ice, which depends on how the glacier accumulation area ratio changes in the future. Similarly, using daily versus monthly climate data can have opposite effects on different glaciers. Our study highlights the importance of considering minor model design differences to predict future glacier volumes and runoff accurately. However, the lack of independent observations limits our ability to evaluate the added value of additional model complexity.

Glacier projections sensitivity to temperature-index model choices and calibration strategies

Lilian Schuster[1], David R. Rounce[2], Fabien Maussion[1]

[1] *Department of Atmospheric and Cryospheric Sciences, University of Innsbruck, Innsbruck, Austria*

[2] *Department of Civil and Environmental Engineering, Carnegie Mellon University, Pittsburgh, PA, United States*

Correspondence: Lilian Schuster <lilian.schuster@uibk.ac.at>

ABSTRACT. Glacier models contribute significantly to the uncertainty of glacier change projections. In this study, we focus on temperature-index mass-balance (MB) models and their calibration, exploring the impact of various design choices on projections. Using the Open Global Glacier Model (OGGM), we compare the effects of different surface-type dependent degree-day factors, temporal climate resolutions (daily, monthly) and downscaling strategies (temperature lapse rates, temperature and precipitation correction) on projections for 88 glaciers with in-situ observations. Our analysis shows that higher spatial and temporal resolution MB observations lead to more accurate MB gradient representations thanks to an improved calibration. Some choices have systematic effects. For example, weaker temperature lapse rates result in smaller glaciers in a warmer climate. However, we often find nonlinear effects, such as with the sensitivity to different degree-day factors for snow, firn, and ice, which depends on how the glacier accumulation area ratio changes in the future. Similarly, using daily versus monthly climate data can have opposite effects on different glaciers. Our study highlights the importance of considering minor model design differences to predict future glacier volumes and runoff accurately. However, the lack of independent observations limits our ability to evaluate the added value of additional model complexity.

1 INTRODUCTION

Current glacier retreat is unprecedented considering the last 2000 years (IPCC, 2021). Global glacier mass loss is projected to continue into the 21st century in response to climate change and is linearly related to temperature change (Rounce and others, 2023; Edwards and others, 2021). Glaciers have been and will continue to be a major source of sea level rise in the 21^{st} century (e.g. Church and others, 2013; Frederikse and others, 2020; Edwards and others, 2021). Furthermore, glaciers are important regulators of water availability in many regions of the world (Kaser and others, 2010; Huss and Hock, 2018) and glacial runoff can potentially buffer future droughts even in regions where runoff declines over the 21st-century (Ultee and others, 2022).

Improving glacier evolution models is thus critical to better understand how glaciers will respond to climate change and improve predictions of corresponding impacts. By partitioning various sources of uncertainty, the Glacier Model Intercomparison Project Phase 2 (GlacierMIP2, Marzeion and others, 2020) found that the primary source of uncertainties of our projections in the first half of the century comes from differences in the glacier models. However, the study could not disentangle the choices in model design nor the specific processes responsible for these variations between glacier models. In our study, we will focus on a central component of glacier evolution models (Zekollari and others, 2022): the mass-balance (MB) model and its calibration.

Most large-scale glacier models (9 out of 11 models in GlacierMIP2) use only temperature and precipitation climate data. Accumulation is estimated by snowfall (i.e., precipitation below a certain temperature threshold) and ablation by temperature-index models (e.g. Braithwaite and Olesen, 1989), where melt is computed by multiplying a calibrated degree-day factor by the sum of temperatures above a chosen threshold. This simple but reliable approach is still prevalent due to significant uncertainties in the local climate forcings and a lack of temporally and spatially-resolved MB observations that would be necessary to calibrate the free parameters from more complex MB models.

The temperature-index models (in the following referring to the ablation and accumulation part of the MB model) used in the literature vary based on their temporal resolution, climate downscaling approaches, representation of surface conditions and the processes that are explicitly modelled. While some temperature-index models of large-scale studies use monthly climate data (Marzeion and others, 2012; Maussion and others, 2019; Rounce and others, 2020b), others also include the daily temperature standard deviation (Huss and Hock, 2015; Anderson and Mackintosh, 2012; Zekollari and others, 2019). Recent General Circulation Models (GCMs) (e.g. ISIMIP3b, Lange, 2019) provide daily data, opening opportunities to evaluate the impact of temporal resolution on glacier projections. Some models use different degree-day factors for different surface types (e.g. snow, firn, ice, and debris cover; Radić and others, 2014; Huss and Hock, 2015; Zekollari and others, 2019; Rounce and others, 2020b,a; Compagno and others, 2022), while others do not (Marzeion and others, 2012; Maussion and others, 2019). Distinguishing surface types is more realistic, as the degree-day factor of snow is generally smaller than that of ice to account for the difference in albedo (e.g. Braithwaite, 2008); however, this distinction introduces more unknown parameters. Additionally, using two or three surface types may not realistically represent the continuous evolution of albedo during the summer melt (Marshall and Miller, 2020). To our knowledge, no systematic comparison of these temperature-index model variants has been performed for data-scarce situations typical of large-scale studies where hundreds or thousands of glaciers are considered at once.

In previous model intercomparisons, the calibration data also varied considerably by model, ranging from using in-situ direct glaciological observations from the WGMS (2020) for about 300 glaciers (e.g. Marzeion and others, 2012; Maussion and others, 2019; Shannon and others, 2019) to regional mean satellite geodetic MB estimates (e.g. Anderson and Mackintosh, 2012; Huss and Hock, 2015; Sakai and Fujita, 2017). The different methods used to extrapolate the calibrated parameters between glaciers result in large uncertainties (e.g. Maussion and others, 2019). Using glacier-specific, instead of regional, mean geodetic MB estimates can capture sub-regional spatial variability and offers unprecedented opportunities for model calibration (Rounce and others, 2023; Compagno and others, 2021; Zekollari and others, 2019; Rounce and others, 2020b). The global geodetic glacier dataset of Hugonnet and others (2021) provides a mean specific glacier MB estimate between 2000 and 2019 for almost every glacier on Earth ($>200\,000$ glaciers). However, these geodetic estimates provide decadal averages and thus do not capture seasonal and/or interannual variations. Our findings suggest that often considered small changes in the model design, such as variations of temperature-index models and calibration options, can influence performance as well as volume and runoff projections. By changing only one model option at a time within the OGGM framework, we provide insight into glacier model behaviour differences that are not possible with large-scale glacier model intercomparison projects.

Since glacier evolution models have multiple model parameters, the use of a single observation per glacier for calibrations causes the model to be overparameterised (Rounce and others, 2020b). This problem is usually ignored by either fixing global parameters (Marzeion and others, 2012; Maussion and others, 2019) or by selecting parameter values sequentially in order of subjectively chosen importance (Huss and Hock, 2015; Zekollari and others, 2019; Compagno and others, 2021). A first attempt to estimate the uncertainty arising from overparameterisation was implemented in Rounce and others (2020a,b) using an empirical Bayesian inverse model, which has the advantage of taking both the overparameterisation and observational uncertainties into account. At the glacier or basin scale, uncertainties originating from overparameterisation can be large, illustrating the need for more observational constraints. Recent advances may soon enable calibration frameworks to use regional to global estimates of elevation-dependent mass balance (Miles and others, 2021) and/or interannual and seasonal mass balance (Jakob and others, 2021). Our study provides insights into the future potential of model calibration based on soon-to-be available data sources.

We aim to methodically evaluate the influence of individual model design choices on both the calibration procedure and glacier change projections. Specifically, we aim to determine the potential added value of more complex temperature-index model variants over simpler and less parameterised approaches. This added value will be evaluated in the context of the amount of calibration data usually available for large-scale studies, as well as in the context of physical plausibility and future glacier response to climate change. Our model choices include the temporal resolution of climate data (monthly or daily), downscaling strategies (near-surface temperature lapse rates as well as temperature and precipitation bias corrections), and surface-type dependent degree-day factors.

We focus on 88 glaciers with long-term observations of annual, seasonal and, in some instances, elevation-dependent climatic mass balance from the WGMS (2020). The various temperature-index model variants and calibration procedures are implemented into the Open Global Glacier Model framework (OGGM), which is well adapted for such a model intercomparison study thanks to its modular structure.

2 INPUT DATA AND METHODS

2.1 Model setup and climate data

We implemented the new MB models within the open-source numerical framework OGGM (Maussion and others, 2019), which has been used in several global and regional studies (e.g. Tang and others, 2023; Furian and others, 2022; Yang and others, 2022; Gangadharan and others, 2022; Li and others, 2022, for most recent examples). Here, we focus on the changes made to OGGM's default configuration as of version 1.5.2. For this study, OGGM uses glacier outlines from the Randolph Glacier Inventory (RGIv6.0, Pfeffer and others, 2014) and a digital elevation model to derive elevation-band flowlines (as in Huss and Farinotti, 2012; Werder and others, 2020). We favoured elevation-band flowlines over multiple geometrical centerlines (also available in OGGM) as they are computationally cheaper and simplify the calibration.

The W5E5v2.0 climate dataset (Lange and others, 2021) is used for the historical period of 1979-2019, while the five primary GCMs from phase 3b of the Inter-Sectoral Impact Model Intercomparison Project (ISIMIP3b, Lange, 2019, 2022) are used for the future period of 2020-2100. The chosen GCMs are based on phase 6 of the Coupled Model Intercomparison Project (CMIP6, Eyring and others, 2016). Downscaled temperature and precipitation data from the nearest gridpoint are used to force the MB model for each elevation band (more in Sect. 2.2).

Both W5E5 and ISIMIP3b are available in daily resolution and have a spatial resolution of 0.5° over the entire globe. Generally, GCMs have to be bias-corrected to approximately coincide with the climate dataset used for model calibration during the common time period. In this study, we did not apply an additional bias correction to match the mean and standard deviation over the largest common period, as the statistically downscaled GCMs from ISIMIP3b are already internally bias-adjusted to W5E5 over the period 1979-2014 (Lange, 2019). Additionally, the bias adjustment from ISIMIP3b is more robust for extreme values than the "delta"-method that is commonly used in OGGM and other models (e.g. Zekollari and others, 2019) as GCMs from ISIMIP3b preserve trends across quantiles (Lange, 2019) and are specifically more reliable for daily climate data. For projections, we run the five GCMs from ISIMIP3b but only show the median of the five simulations for the various model options, as multi-GCM uncertainty is not a focus of this study. We run the simulations for two Shared Socioeconomic Pathways (SSPs): the low-emission scenario SSP1-2.6 and the very high-emission scenario SSP5-8.5, which correspond to a global temperature increase by 2100 compared to preindustrial times of 1.7°C and 4.6°C and a global glacier area-weighted temperature increase of 3.1°C and 8.0°C, respectively.

Glacier dynamics are represented by a 1D shallow-ice flowline model in OGGM assuming a trapezoid bed shape. Ice thickness is estimated by applying the mass-conservation approach (Farinotti and others, 2009, 2019; Maussion and others, 2019) and assumes the glacier outline and digital elevation model have the same date. For this study, we calibrate the creep parameter A individually for each glacier to match the ice volume estimates of Farinotti and others (2019) at the RGI year (for many glaciers close to 2000). More details about the OGGM are available on the model documentation website (`http://docs.oggm.org`) and in Maussion and others (2019).

2.2 Temperature-index model options

The model options presented in this study are variations of the original temperature-index model of OGGM presented in Maussion and others (2019). The (monthly or daily) mass balance B_i at an elevation z is estimated as

$$B_i(z) = P_i^{solid}(z) - d_f(snow/ice) \cdot \max(T_i(z) - t_{melt}, 0) \tag{1}$$

where $P_i^{solid}(z)$ is the solid precipitation ($\mathrm{kg\,m^{-2}\,month^{-1}}$ or $\mathrm{kg\,m^{-2}\,day^{-1}}$), T_i the air temperature (°C) and t_{melt} the temperature threshold above which melt is assumed to occur (in this study: 0 °C, i.e., different from the OGGM default of -1 °C). d_f is the degree-day factor of a specific surface type ($\mathrm{kg\,m^{-2}\,K^{-1}\,month^{-1}}$ or $\mathrm{kg\ m^{-2}\ K^{-1}\ day^{-1}}$). The fraction of solid precipitation is estimated from the monthly or daily mean temperature. Precipitation is assumed to be entirely solid below 0 °C and all liquid above 2 °C. In between, the solid precipitation proportion changes linearly.

The temperature-index model variants all have at least three free parameters. Besides the degree-day factor, which can vary for different snow ages and ice, two parameters are often considered as part of the MB model but are, in fact, local climate downscaling or bias correction tools. Precipitation is corrected by a fixed multiplicative scaling precipitation factor (p_f) and temperature by a temperature bias (t_b). Without the precipitation factor or temperature bias, the observed glacier MB can often not be reproduced by the model. These model parameters are not purely downscaling parameters. All MB model parameters account for local climate biases, missing MB processes (debris cover, avalanches ...) or erroneous MB observations (see Rounce and others, 2020b). As commonly done in large-scale studies and to not complicate the matter further, these parameters are assumed to be constant over the years.

In total, we explore 18 combinations of temperature-index model variants (Table 1), which are all available to OGGM users (see Code & Data availability section).

Temperature lapse rate choice

The temperature is adjusted to the flowline gridpoint altitude by a lapse rate. We set the temperature lapse rate either to (i) a constant value ($-6.5\,\mathrm{K\,km^{-1}}$, reference option in OGGM) or (ii) extract it from pressure levels in ERA5 so that it is variable spatially and seasonally (i.e., we apply twelve constant monthly temperature lapse rates as in Marzeion and others, 2012; Huss and Hock, 2015; Rounce and others, 2020a). Note that we do not apply any precipitation gradient.

Table 1. Temperature-index model options used in this study, summing to 18 combinations. The simplest combination (constant temperature lapse rate, monthly climate data, and no surface-type distinction) is used as reference.

Model option	Option name	Details
Temperature lapse rate	*constant*	*reference, -6.5 K km*$^{-1}$
	variable	spatially & seasonally variable, but the same over the years, derived from ERA5
Temporal climate resolution	*monthly*	*reference, monthly temperature and precipitation*
	pseudo-daily	superimposed daily temperatures from daily standard deviation (spatially & seasonally variable, but the same over the years), monthly precipitation
	daily	daily temperature & precipitation
Surface type distinction	*no*	*reference, mixed snow-ice degree-day factor (*d_f*) used*
	yes (neg. exp.)	negative exponential increase of snow d_f with snow age, ice d_f applied after six years, $d_{f,\,fresh\,snow}$=$d_{f,\,ice} \cdot 0.5$, see Appendix Fig. 8
	yes (linear)	linear increase of snow d_f with snow age, everything else same as in neg. exp.

Temporal climate resolution choice

Air temperature and precipitation data are used to force the model. We have three options for the climate data based on the temporal resolution and variability (Table 1): (i) monthly data, (ii) pseudo-daily data, (iii) daily data. The monthly option is the simplest, while the advantage of pseudo-daily and daily options is that melt can occur even if the monthly mean temperature is below 0°C.

Variants of the pseudo-daily option are currently in use by large-scale temperature index model applications (Huss and Hock, 2015; Zekollari and others, 2019), while the daily option is less used (Anderson and Mackintosh, 2012) due to data availability. The pseudo-daily approach assumes that daily temperatures are normally distributed over the month. A quantile method is used to sample the normal distribution in a reproducible way to estimate the monthly melt. For a better comparison, we use a similar method as in past applications (e.g. in Huss and Hock, 2015). The same daily temperature standard deviation computed from the past climate (here: 2000-2019) is applied to future climate (i.e., we apply twelve constant daily standard deviations over the entire period). Note that in a warming world, the pseudo-daily approach will likely overestimate daily temperature standard deviations as temperature variances are expected to decrease (specifically in the Northern Hemisphere winter, Screen, 2014; Tamarin-Brodsky and others, 2020).

The daily option estimates solid precipitation from the daily temperature, while the monthly and pseudo-daily options estimate the solid precipitation from the monthly mean temperature. Hence, the monthly and pseudo-daily approaches will have the same amount of solid precipitation but different melt amounts, while the daily option will have different amounts of melt and solid precipitation compared to the monthly option.

Surface-type distinction choice

Over snow and firn surfaces, less melt occurs for the same temperature compared to bare ice surfaces due to differences in albedo (e.g. Braithwaite, 2008). We track snow age with a new snow ageing bucket system (see Appendix A.1 for more detail) to distinguish between snow, firn, and ice at each elevation band, thereby enabling the use of different degree-day factors for these surface types. We assume a degree-day factor ratio of 0.5 between new snow and ice (as in Huss and Hock, 2015; Zekollari and others, 2019) but acknowledge that this is arbitrary (Rounce and others, 2020a). As the snow ages, we assume the ratio of the older snow to the ice degree-day factor increases every month, i.e., the assumed ratio of 0.5 is only applied for new snow and transitions to 1 over six years (i.e., the snow becomes ice). The speed of how the degree-day factor transitions from snow to ice surfaces is not well known.

We therefore compare three approaches to determine the impact on model performance and glacier projections: (i) no degree-day factor change, (ii) a negative exponential increasing degree-day factor with snow age where 63% of the changes occur in the first year or (iii) a linearly increasing degree-day factor with snow age (Appendix Fig. 8d). An argument for using an exponential degree-day factor transition with time is that Marshall and Miller (2020) found a linear relationship between degree-day factor and albedo, and albedo can be parameterised to decay exponentially with time.

2.3 Geodetic and in-situ mass balance observations

The main MB observations used for calibration are the geodetic estimates from Hugonnet and others (2021) as they are globally available and presently the primary reference for global studies (Rounce and others, 2023). However, higher spatially and temporally resolved in-situ direct glaciological observations exist from the WGMS (2020) for around 300 glaciers. In the period of the applied climatic dataset (1979-2019), estimates of interannual MB variability of at least 10 years exist for 180 glaciers, and winter MB observations of at least five years exist for 118 glaciers. There are 95 glaciers with both sufficient winter MB and interannual MB variability data. MB profile data (with at least five years and five elevation

Table 2. Calibration options for glaciers with additional in-situ direct glaciological measurements from the WGMS (2020). "Cal" means that this parameter is calibrated glacier-specifically, and "x" means this observational target variable is used and matched. d_f stands for degree-day factor, p_f for precipitation factor, t_b for temperature bias, prcp. for precipitation and std. for standard deviation. For C_4 and C_5, some in-situ observational data are used for pre-calibration; they are therefore marked as "indirect". When comparing the options, we use only the 88 glaciers that can be calibrated for all options and all temperature-index models given the assumed parameter ranges.

options & glaciers used		parameter value			target variable (for calibration)		
		d_f	p_f	t_b	geodetic mean	winter MB mean	annual MB std.
C_1	n=95	cal	cal	cal	x	x	x (±10%)
C_2	n=118	cal	cal	0	x	x	-
C_3	n=180	cal	cal	0	x	-	x
C_4	n=247[a]	cal	constant, median of C_3	0	x	-	(indirect)
C_5	n=247[a]	cal	F(winter prcp.), cal by C_2	0	x	(indirect)	-

[a]could also be applied on worldwide glaciers as it only uses the glacier-specific geodetic estimate

bands) exist for only 93 glaciers. We will show that these additional observations can be used to calibrate a glacier-specific precipitation factor and/or temperature bias alongside the degree-day factor for these glaciers (see Fig. 1).

2.4 Mass-balance model calibration options

We developed five calibration options for glaciers with additional in-situ data to calibrate the three free parameters (Table. 2). We set the allowed ranges of the degree-day factor to $0.33-33\,\mathrm{kg\,m^{-2}\,K^{-1}\,day^{-1}}$, precipitation factor to $0.1-10$, and temperature bias to -8 − 8 K. All five options calibrate the MB model to match the 20-year average glacier-specific geodetic observation (2000-2019) from Hugonnet and others (2021). Two options also use the mean winter MB (C_1, C_2), and two options use the interannual variability (standard deviation) of annual MB (C_1, C_3). The precipitation factor varies on a glacier-per-glacier level for all options except for C_4, and the temperature-bias is non-zero only for C_1. For C_4, we use a different precipitation factor for every temperature-index model option, which is set to be constant for all glaciers (median precipitation factor from C_3). For C_5, the precipitation factor depends on the glacier's winter precipitation based on a logarithmic relation found from option C_2 between winter precipitation and glacier-specific precipitation factor (Fig. S1a). This correction is arguably more reasonable than a constant precipitation factor because locations with a high baseline precipitation value are not corrected towards unrealistic amounts (Fig. S1b). The precipitation factor in C_5 can be different for every glacier but is the same for every temperature-index model option (Fig. 2e).

Lower calibration option numbers use more observational data, thus reducing the number of glaciers that can be investigated due to calibration data availability. We found that the precipitation factor influences interannual MB variability and winter MB more than the temperature bias (e.g. Fig. 1). Therefore, we decided that calibration options C_2 and C_3 have a variable precipitation factor but do not apply any temperature bias. Option C_4 is similar to how the precipitation factor was calibrated in OGGM, and option C_5 is the new way of calibrating the precipitation factor (upcoming OGGM v1.6). All glaciers worldwide could be calibrated using C_4 and C_5.

Since we want to model the total MB to assess the impacts of glacier change (e.g. seasonal runoff and sea level rise), all calibration and MB model options are tuned to match the total MB (i.e., average geodetic MB) and not the in-situ average climatic MB (the two are sometimes inconsistent for numerous reasons, e.g. Klug and others, 2018). The in-situ data is primarily used for estimates of the interannual variability, altitude-dependant MB profile, and winter MB.

In total, 88 of 95 potential glaciers with available data could be calibrated for all five calibration options and all temperature-index model options when using the applied parameter ranges. We will compare the different options on these 88 glaciers, of which 84 come from the Northern Hemisphere (28 from Central Europe and 19 from Scandinavia, see Fig. S2). The MB profile data is only available for 53 out of the 88 glaciers and has large uncertainties, so we only use it as an independent validation measure (see below). Note that an accurate MB profile leads to improved ice thickness estimates in mass-conserving inversion methods such as OGGM (Maussion and others, 2019) and likely influences future glacier volume.

2.5 Model option comparison methods

The performance of the MB model and calibration options is assessed by estimating how well they match the MB profile in terms of the mean MB gradient absolute bias below the equilibrium line altitude and the mean absolute error to the average altitude-dependent MB. We estimate the MB profile performance compared to calibration option C_1 for all 18 MB model combinations for the 53 glaciers that could be calibrated and had observed MB profile data. For the MB model options, we compare the performance to the reference MB model using solely calibration option C_5. We compare the agreement between the modeled and observed MB profile for 80 glaciers and the annual MB variability (independent dataset for C_5, Table 1) for 212 glaciers. We also chose option C_5 for the MB model performance comparison, as C_5

(and C_4) can be applied to glaciers globally.

Differences in projected glacier volumes are analysed by dividing the individual glacier volumes for various MB model options against the reference MB model options or for the various calibration option compared to C_1 for the years 2040 and 2100. This comparison could only be made for glaciers where no option projects a total glacier disappearance, which was the case for 45 out of 85 glaciers for SSP1-2.6 and 15 glaciers for SSP5-8.5. We analyse general tendencies that are true no matter which set of options we choose. For the MB model choice, we thus compare the influence of a specific MB model choice (e.g. daily vs monthly temporal resolution) compared to all other MB models and all five calibration options together. Similarly, we evaluate the influence of a specific calibration option by comparing all 18 MB model options together. Additionally, we assess whether one calibration option results in more or less spread between the different MB model options by estimating the volume ratios of any option versus the reference MB model for the years 2040 and 2100. The distribution of the standard deviation of the MB model option volume ratios (i.e., each glacier has a standard deviation) is used to compare how much the MB model types vary for each calibration option for 2040 and 2100.

3 FIXED-GEOMETRY MASS-BALANCE

In this section, we explore the influence of the calibration and MB model options on the MB model output assuming a constant glacier area as of the RGI date, i.e., we do not update the glacier geometry and thus do not account for additional glacier geometry and elevation feedbacks to better isolate the differences between options.

3.1 Influence of overparameterisation on the temperature-index model output

Despite the simplicity of the temperature-index model, overparameterisation from downscaling model parameters strongly influences the MB variability and gradient. We show these effects in Fig. 1 for a typical case of a large-scale glacier modelling study, where only one observation is available. Building upon Rounce and others (2020a), we vary either the precipitation factor or temperature bias while always matching the geodetic MB and analysing corresponding changes in the modeled MB interannual variability and MB profile.

An increase in the precipitation factor results in a linear increase in the degree-day factor (Fig. 1a, Eq. 1). More annual precipitation results in more solid precipitation and a higher winter MB (Fig. 1e),

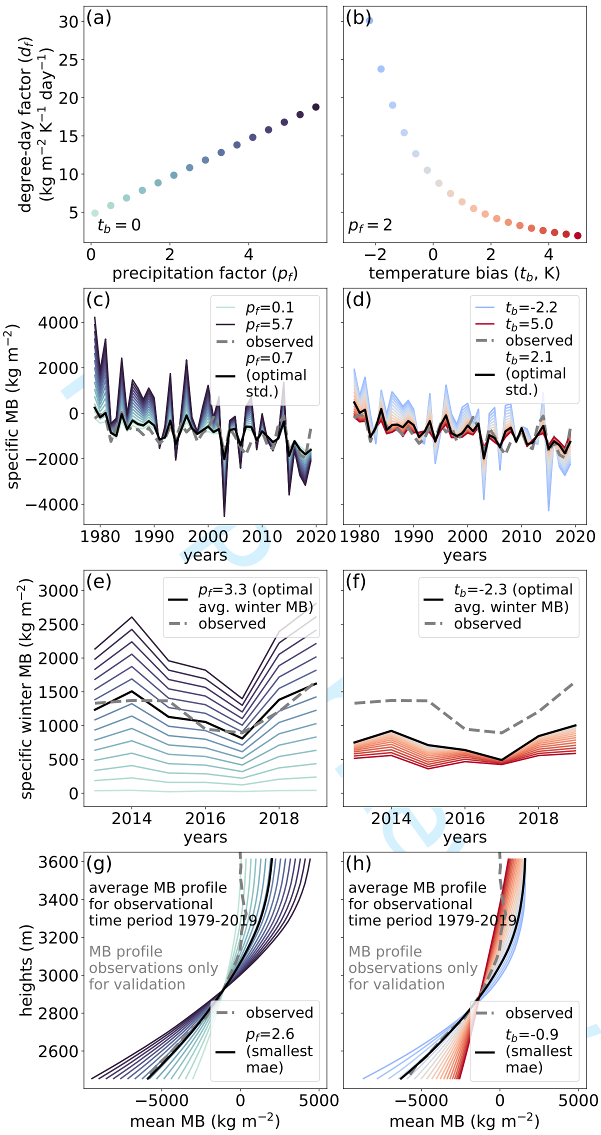

Fig. 1. Influence of downscaling MB model parameters on the calibrated **(a, b)** degree-day factor (d_f) to match the geodetic observations and on the resulting **(c, d)** interannual MB variability, **(e, f)** average winter MB and **(g, h)** mean elevation-dependent MB profiles. Although all parameter combination choices can match the mean specific MB equally well, they differ in the other measures. On the left plots, **(a, c, e, g)**, temperature bias (t_b) is set to zero and precipitation factor (p_f) is varied while on the right plots, **(b, d, f, h)**, p_f is set to 2 and t_b is varied. std stands for standard deviation, mae for mean absolute error. The shown estimates & observations are for the Hintereisferner glacier, Ötztal Alps, Austria using the reference MB model option. Each of the d_f, p_f and t_b combinations match the one geodetic mean observation. Combinations that best match the in-situ observations are indicated.

which is balanced by more melt to match the observed geodetic MB. The larger precipitation and degree-day factors also lead to a roughly linear increase of the interannual MB variability (Fig. 1c), as the multiplicative parameters amplify precipitation and temperature anomalies of the climate time series. The larger precipitation factor also causes a larger MB gradient, with more solid precipitation at the top and more melt at the bottom of the glacier (Fig. 1g).

Increasing the temperature bias and keeping the precipitation factor constant, in turn, results in a logarithmic decay of the degree-day factor (Fig. 1b). Lower temperatures reduce the likelihood of crossing the melt threshold and increase the likelihood of crossing the solid precipitation threshold (Eq. 1), resulting in this nonlinear behaviour. Lower temperature biases (and higher degree-day factors) also cause a logarithmic increase in the interannual MB variability (Fig. 1d). However, the influence on total variance is smaller than that of higher precipitation factors (Fig. 1c) because the degree-day factor only affects the melt rates and the temperature bias has a limited impact on accumulation rates. Winter MB decreases only slightly with increasing temperature; an effect that becomes more substantial for larger temperature biases (Fig. 1f). Therefore, varying the temperature bias does little to help match the observed winter MB. Finally, a positive temperature bias also decreases the MB gradient and makes the MB change with altitude more linear (Fig. 1h), as the reduction of solid precipitation at higher altitudes needs to be compensated by less melt at lower altitudes (i.e., a lower degree-day factor).

3.2 Temperature-index model option influence on calibrated parameter combinations

Due to a complex interplay between MB model parameters, the calibrated parameter combinations vary strongly between the temperature-index model and calibration options. To understand the reasons for the differences in performance and projections, we first show and analyse these model parameter differences based on the 88 glaciers where all options could be calibrated (Fig. 2).

Temperature lapse rate choice

The calibrated degree-day factor is smaller for the variable lapse rate option than the constant option (valid for all calibration and other MB model change options, Fig. 2). The variable lapse rate is, in our case, for most glaciers and months, less negative than the constant option (median of -5.6 $\mathrm{K\,km^{-1}}$ versus -6.5 $\mathrm{K\,km^{-1}}$). Therefore, the glacier is forced with higher temperatures using the variable lapse rate option as the lapse rate is less negative, and the glaciers are usually higher than the climate gridpoint altitudes,

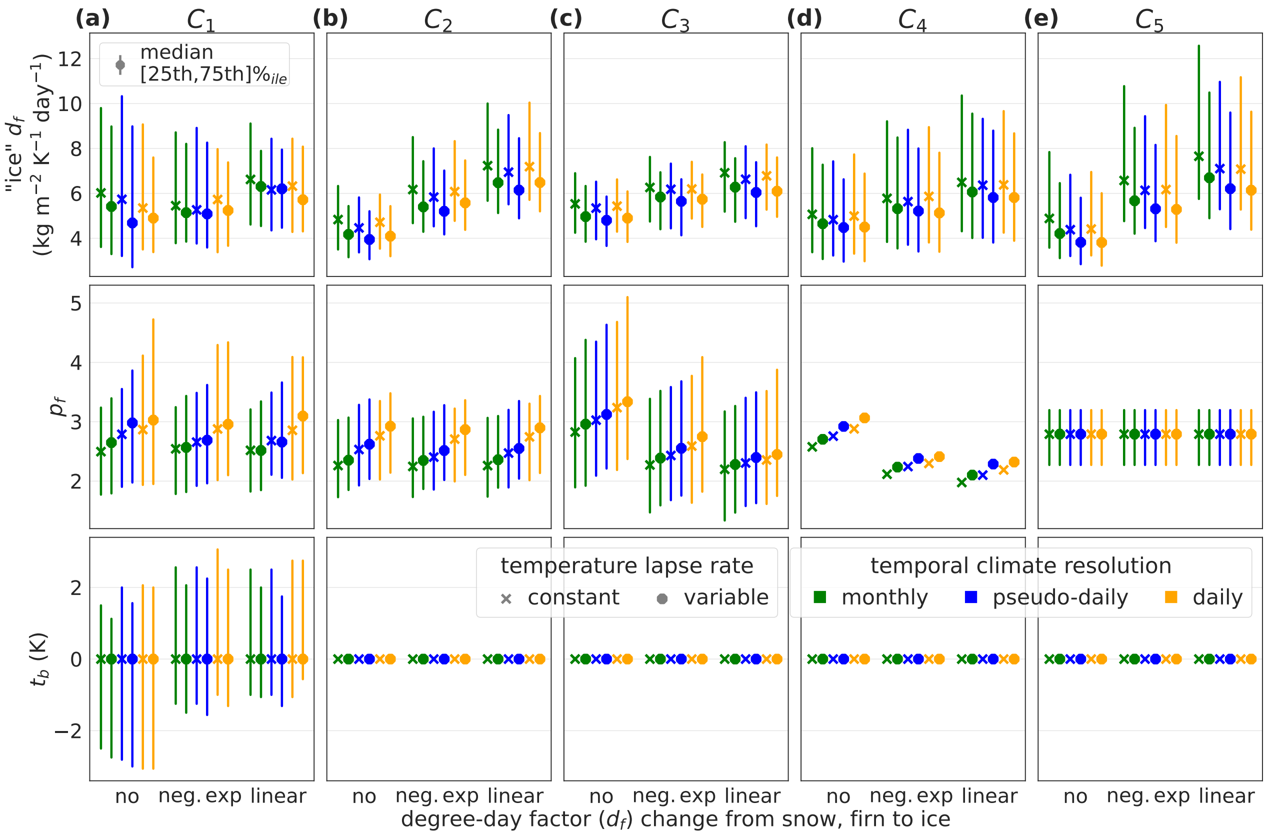

Fig. 2. Calibrated model parameters for different temperature-index model (Table 1) and calibration (Table 2) options C_{1-5}. d_f stands for degree-day factor, p_f for precipitation factor, and t_b for temperature bias. The parameter distributions (median and interquartile range, $25\%_{\mathrm{ile}}$-$75\%_{\mathrm{ile}}$) are shown for the 88 glaciers with enough in-situ observations to apply all calibration options.

which explains the smaller degree-day factors.

When allowed to vary, the precipitation factor is larger for the variable and less negative lapse rates compared to the constant lapse rate. Following Fig. 1a, a smaller precipitation factor would be needed to match the observations if a lower degree-day factor is applied. Thus, the reversed relationship that results in lower degree-day factors for the variable lapse rates compared to the constant lapse rate is not a result of overparameterisation but a result of the higher air temperatures.

Temporal climate resolution choice

For the three temporal climate data options, the degree-day factor is lowest for the pseudo-daily and daily data and highest for monthly data (Fig. 2). We expect a smaller degree-day factor for the pseudo-daily and daily data as melt can occur in these options even if monthly mean temperatures are slightly below the melt temperature threshold. In all calibration options with variable precipitation factors (C_1-C_4, Fig. 2a-d), the theoretically decreased solid precipitation for the daily option is balanced out by a larger precipitation factor to match the average winter MB (Fig. 2b), the interannual MB variability (Fig. 2c) or both (Fig. 2a).

Surface-type distinction choice

If the temperature bias is kept constant at 0, we find that the degree-day factor for the option without surface-type distinction (i.e., for both snow and ice) is lower than the one used for ice in the surface-type distinction models (Fig. 2b-e). This is expected for the options with surface-type distinction since the higher (ice) degree-day factor is only applied for ice surfaces, and a lower degree-day factor (up to a factor of 0.5) is applied for snow or firn surfaces that have a higher albedo than ice surfaces (see Sect. 2.2 & Appendix Fig. 8). When using a snow degree-day factor that increases faster with snow age (using a neg. exp. instead of linear increase), the resulting ice degree-day factor is smaller than in the linear change assumption case. In the neg. exp. case, the degree-day factor will be larger for a few months old snow until a few years old firn than in the linear case due to the faster change in the beginning of the neg. exp. option (Appendix Fig. 8d).

When only matching the winter MB and not applying any temperature bias (C_2), the precipitation factor is almost the same for the three surface-type change options (Fig. 2b). Winter MB depends much more on the precipitation factor than the degree-day factor; thus, the surface-type distinction makes little difference. When matching interannual MB variability (option C_3), a temperature-index model where the degree-day factor changes from snow to firn or ice needs a smaller precipitation factor than one without (Fig. 2c). With surface-type distinction, positive MB anomalies from large (solid) precipitation years are enhanced by the lower snow degree-day factor, and negative MB anomalies are enhanced by using the higher firn or ice degree-day factor. Consequently, if a calibration option uses the same precipitation factor, the interannual MB variability will be larger for models including surface-type distinction.

When having three free parameters (C_1), neither precipitation nor degree-day factor changes consistently between the surface-type options (Fig. 2a). However, the temperature bias changes, which has a similar effect as a higher degree-day factor. A positive temperature bias is applied to balance out otherwise decreased melt for options with surface-type distinction, and a negative temperature bias is applied for those without surface-type distinction (Fig. 2a). Again, this is not a result of overparameterisation, but reflects the parameter combinations which better match all observed variables.

3.3 Temperature-index model performance

We used different temperature-index models where some may reproduce reality better than others. Therefore, we assess whether we can find an added value in these models by comparing modelled MB to independent validation data (Fig. 3, Fig. S3–5).

The modelled MB gradient below the equilibrium line altitude (ELA) is larger when using a constant instead of a variable (mostly less negative) temperature lapse rate (Fig. S4). Larger temperature changes along the glacier due to higher lapse rates increase the melt in the ablation area and the solid precipitation in the accumulation area. Using the constant lapse rate option coincides better with observed MB gradients below the ELA in combination with the no surface-type distinction options. At the same time, the constant lapse rate option results in worse performance in combination with surface-type distinction (Fig. 3a). When including surface-type distinction, we get a larger MB gradient below the ELA (Fig. S4) due to the different applied degree-day factors of snow and ice (specifically true for the linear changing case, see the MB profile comparison for an example glacier in Appendix Fig. 8d). As a result, using less negative (variable) temperature lapse rates that decrease the MB gradient below the ELA and applying surface-type dependent degree-day factors that increase the MB gradient below the ELA balance out each other. Both result in a similar gradient and, thus, a similar performance compared to the reference MB model option (Fig. 3a).

There is no clear tendency in the MB gradient below the ELA for the different temporal climate

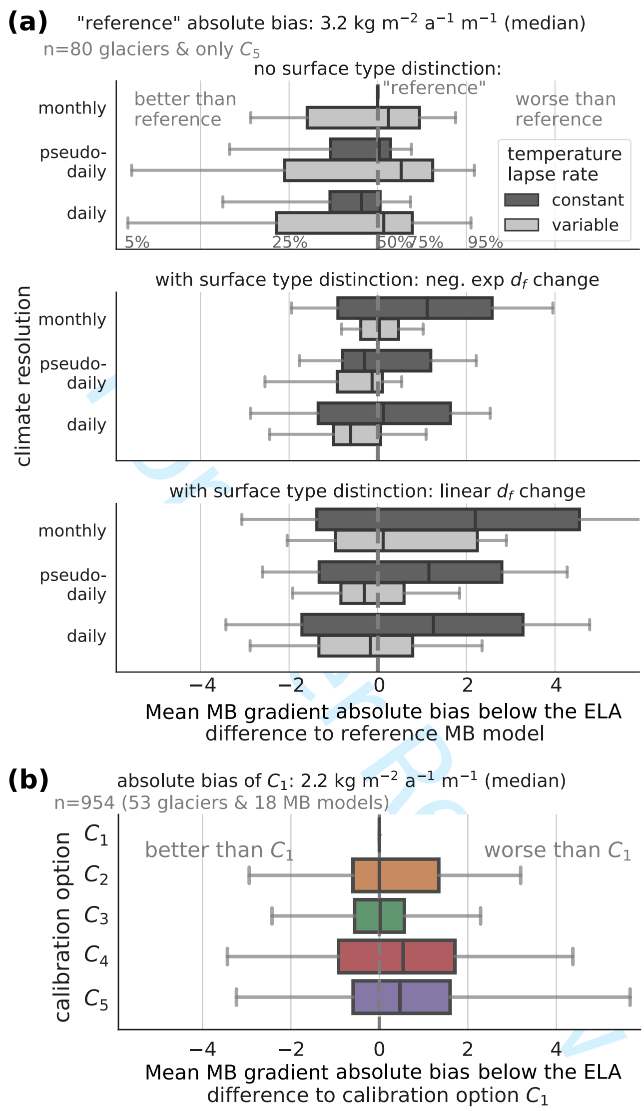

Fig. 3. Performance comparison from independent observations. The difference in the mean MB gradient absolute bias below the equilibrium line altitude (ELA) is shown for **(a)** different MB models and **(b)** different calibration options. Note that the comparisons in (a) are only from C_5 and for 80 glaciers, while in (b), distributions represent general tendencies from all 18 MB model options and 53 glaciers. In (a), the median measure from the reference model using C_5 is compared to the other MB model options. In (b), the median measure of all MB models of options using C_1 is compared to the other calibration options. The resulting distributions are represented by the $5\%_{\text{ile}}$, $25\%_{\text{ile}}$, $50\%_{\text{ile}}$ (median), $75\%_{\text{ile}}$ and the $95\%_{\text{ile}}$. A distribution shift to the right means, for each measure, that this option matches the validation measure worse than the reference option or C_1. d_f stands for degree-day factor. Further performance measures of the MB models are in Fig. S5 and of the calibration options in Fig. S6.

resolution options (Fig. 3a) as there is also no systematic influence of the temporal resolution on the MB gradient below the ELA (Fig. S4). However, pseudo-daily or daily matches the observed MB gradient below the ELA better in combination with a model with surface-type distinction and a variable (less negative) lapse rate.

The MB model performance based on the MB profile mean absolute error ratios are similar to those from the mean MB gradient absolute bias below the ELA (Fig. S5a). However, the differences in how well the MB model options match the observed interannual MB variability are smaller (Fig. S4b). Nevertheless, the MB model combinations that performed worse for the MB profile match (i.e., monthly, constant, with surface-type distinction) also performed worse in matching the annual MB variability (Fig. 3a, Fig. S5).

3.4 Calibration option performance

Some calibration options use more data than others, enabling us to assess whether this improves the model performance (Fig. 3b, Fig. S6). There is a clear tendency that including more observational data for calibration results in a better match with the observed MB profile (the only validation data for all calibration options), i.e., when additionally calibrating the downscaling parameter(s) (p_f & t_b) on a glacier-per-glacier level. However, the observed MB profiles are slightly better matched when the calibration of the degree-day factor and precipitation factor used the interannual MB variability (C_3) instead of the mean winter MB observations (C_2). When using both the interannual MB variability and mean winter MB for calibration (C_1), no further improved performance was found compared to just matching the interannual MB variability (C_3).

3.5 Climate sensitivities of temperature-index model options

Although the MB model options are all calibrated to the same average specific MB, the MB model options create diverging specific MB in a different climate, as their sensitivity to the climate anomalies varies. To isolate these differences, we analyse the direct drivers of temperature-index models similar to Bolibar and others (2022), i.e., cumulative positive degree-days (CPDD) and solid precipitation, on all 217 glaciers under calibration option C_5. We differentiate between temperature-induced and annual precipitation-induced MB anomalies (Fig. 4a,e). We represent their dependence on CPDD, solid winter and summer precipitation anomalies that are induced by these temperature changes (Fig. 4b-d) or annual precipitation changes (Fig. 4f-h). For this synthetic experiment, we assume a fixed area over 20 years and still do not

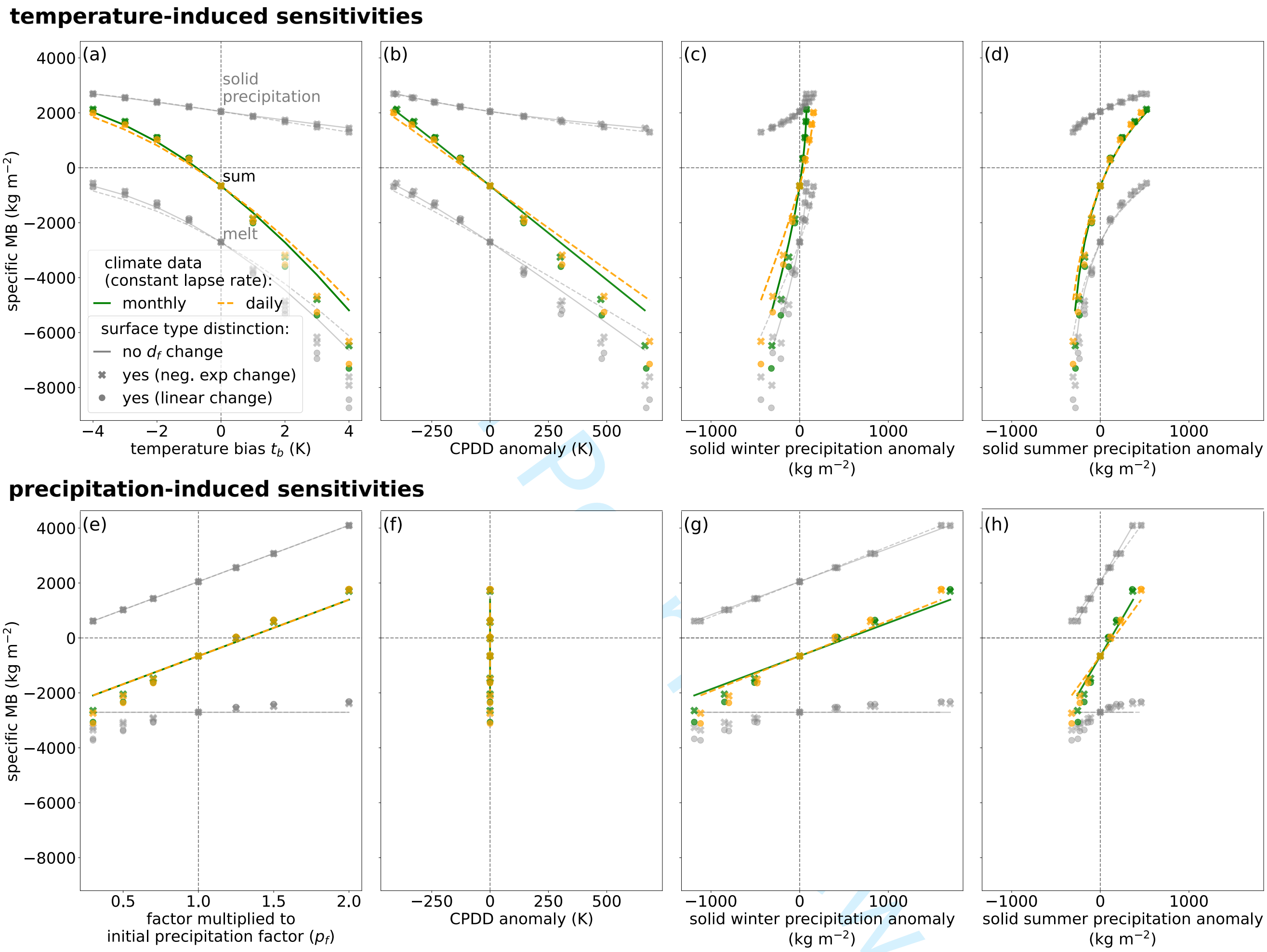

Fig. 4. MB sensitivity of (a-d) temperature and (e-h) precipitation anomalies averaged over the period 2000–2019 on 217 glaciers. (a) Average specific annual MB anomaly dependent on applied temperature bias (t_b), separately for the ablation (melt) and accumulation (solid precipitation) term or both together (sum). In **(b)**, t_b is translated into a cumulative positive degree-day (CPDD) anomaly. As the temperature changes, solid precipitation changes as well. In **(c, d)**, the respective relations of the resulting solid winter and summer precipitation anomaly are shown. In **(e, f, g, h)**, equivalent plots when applying an annual precipitation anomaly solely by a changing precipitation factor (p_f) are shown. The plot is inspired by Bolibar and others (2022, their Fig. 3). Here we use calibration option C_5 because, in that option, p_f of one glacier is the same for all MB models, which facilitates comparisons. d_f stands for degree-day factor.

account for any ice dynamics.

With no surface-type distinction, melt decreases by definition linearly with increasing CPDD, and with that, specific MB increases almost linearly with increasing CPDD (Fig. 4b). However, when applying gradually changing degree-day factors for different surface types, the MB sensitivity becomes nonlinear with increased melt for larger CPDD anomalies because of increasing exposed ice area. With increasing temperatures, the solid precipitation also decreases (Fig. 4a, b). Consequently, the specific MB also strongly decreases as a result of temperature-induced negative solid precipitation anomalies, which is further enhanced with surface-type distinction (Fig. 4c, d). Temperature-induced negative solid winter or summer precipitation anomalies correlate in our experiment with decreasing total solid precipitation and, thus, with increasing melt.

Applying a negative temperature anomaly results in only a small increase in solid winter precipitation (Fig. 4c), since winter precipitation is primarily solid already. For that reason, the specific MB increase of temperature-induced solid winter precipitation is mainly a result of reduced melt and increased solid summer precipitation. The change in specific MB with temperature-induced positive solid summer precipitation anomalies behaves the other way around (i.e., a reversed curve shape, Fig. 4d) with decreasing MB sensitivities for increased temperature-induced solid summer precipitation. The reason is likely that the solid summer precipitation contribution to MB increases faster than other dominant drivers of increased MB, i.e., less melt and increased solid winter precipitation.

Annual precipitation anomalies without temperature change influence solid precipitation, and if the degree-day factor is surface-type dependent, it also influences the melt but not the CPDD (Fig. 4e, f). The otherwise linear increase of specific MB with precipitation-induced solid precipitation increase becomes nonlinear when applying a surface-type dependent degree-day factor (Fig. 4g, h). Due to the increased melt of ice surfaces, the divergence between the MB models increases for decreasing solid precipitation.

Consequently, the relationship between specific MB and solid precipitation depends on the driver of the solid precipitation anomaly (temperature or precipitation change) and whether other anomalies are correlated to it. The relation is much stronger, nonlinear and varies between the seasons for all MB model options in case of a, likely more realistic in a future climate, temperature-induced anomaly (Fig. 4d, e) than in case of a precipitation-induced anomaly (Fig. 4g, h). The larger negative MB for stronger negative solid precipitation anomalies when including surface-type distinction is, however, the same in both cases.

The temporal climate resolution, for example, also influences the sensitivity. Less melt occurs in the

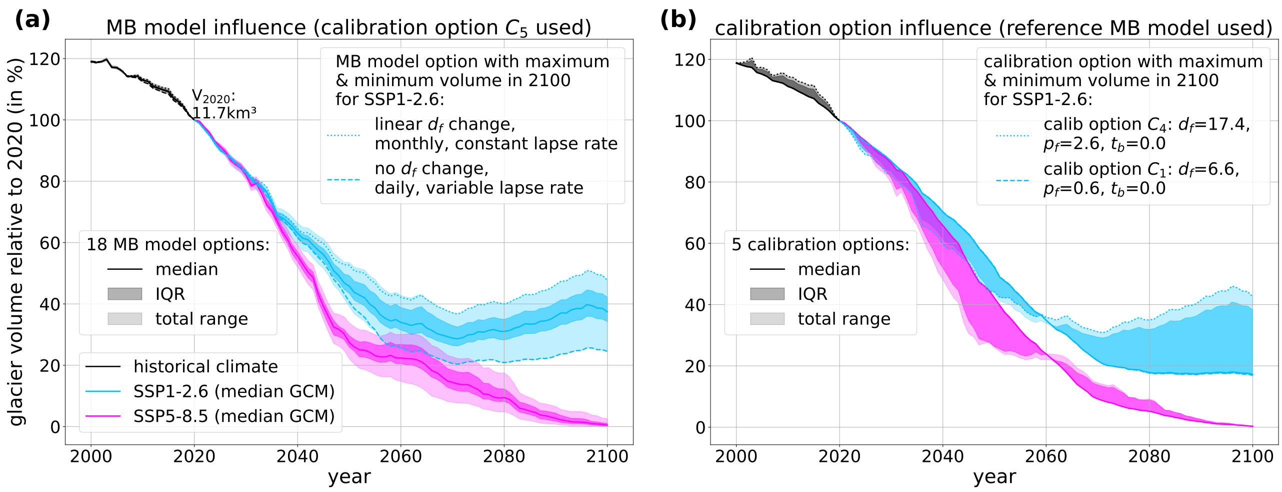

Fig. 5. Aletsch glacier volume projections (2000-2100) for two SSP scenarios. The median, interquartile range (25%ile–75%ile, IQR) and the total range resulting from **(a)** the temperature-index model options using C_5 and **(b)** the calibration options using the reference MB model are shown. Note that for this glacier, in (b), the calibrated parameters and thus projections for options C_1, C_2 and C_5 of the reference MB model are very similar. d_f stands for degree-day factor, p_f for precipitation factor, and t_b for temperature bias. The volume estimates correspond to the median volume from the five GCMs.

daily option for the same temperature bias or CPDD anomaly in case of positive temperature anomalies and vice versa (Fig. 4a, b). The differences result from the new imbalance between the influence of the temperature threshold and the smaller degree-day factor when using daily compared to monthly climate data (Fig. 2e). Additionally, the solid winter precipitation variations from temperature anomalies are stronger in the daily MB model as solid precipitation is estimated daily (Fig. 4c).

4 INFLUENCE ON DYNAMIC GLACIER PROJECTIONS

The comparison to MB profiles in Sect. 3.3 showed a relatively minor difference in performance among model options. Furthermore, the additional data required to properly calibrate all the model parameters are only available for a limited number of glaciers. Therefore, we now assess how small changes in the model design of the temperature-index model and its calibration can influence glacier volume projections outside of the calibration period. We start with a case study of a single glacier projected to not vanish in the course of the century (Aletsch glacier, Fig. 5), and then analyse all non-vanishing glaciers with sufficient calibration data (Fig. 6).

Many glaciers with in-situ observations are melting away quickly, which makes comparisons complicated. From the 85 glaciers considered, approx. 14% of their volume is projected to remain in 2060, relative to

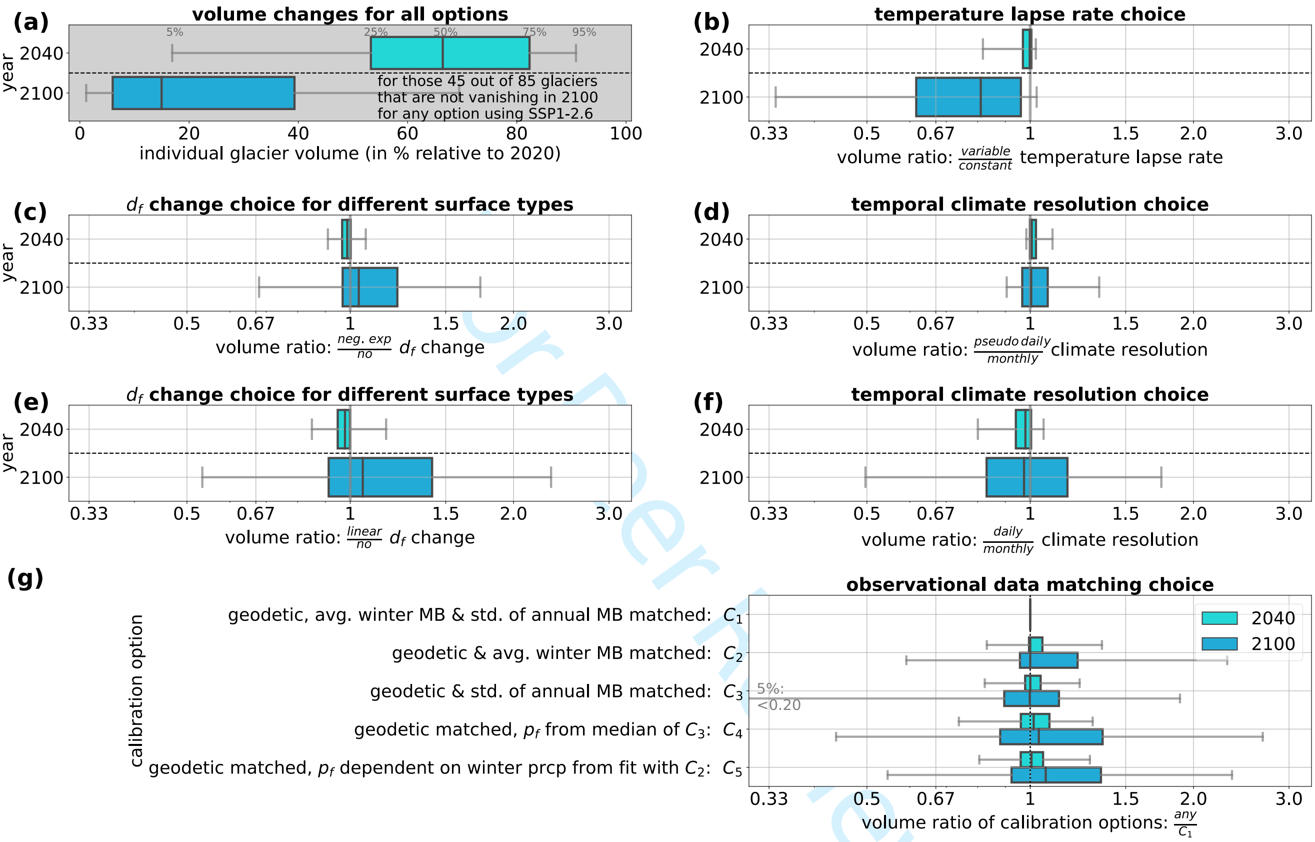

Fig. 6. **(a)** Individual glacier volume changes in 2040 and 2100 for 45 glaciers that could be calibrated on all options and still exist in 2100 under the SSP1-2.6 scenario. Individual glacier volume ratios for **(b-f)** temperature-index model and **(g)** calibration options. The resulting distributions are represented by the $5\%_{\mathrm{ile}}$, $25\%_{\mathrm{ile}}$, $50\%_{\mathrm{ile}}$ (median), $75\%_{\mathrm{ile}}$ and the $95\%_{\mathrm{ile}}$. A distribution shift to the right (left) means that including this option instead of the reference option results in a larger (smaller) glacier volume than the MB model combinations that use the respective reference option. Note that the volume changes and ratios are estimated from all MB model and calibration options, i.e., (a) represents 45 glaciers · 5 calibration · (3 · 3 · 2) MB model options. Volume ratios are in total represented respectively by (b) $45 \cdot 5 \cdot (3 \cdot 3)$, (c–f) $45 \cdot 5 \cdot (3 \cdot 2)$, and (g) $45 \cdot (3 \cdot 3 \cdot 2)$ glaciers and options. The volume estimates correspond to the median volume from the five GCMs. Fig. S8 shows the same for SSP5-8.5.

2020, under the SSP1-2.6 scenario and 4% under the SSP5-8.5 scenario, respectively. For the Hintereisferner glacier, all examined MB models, calibration options, and both SSP scenarios project that 16% or less of the glacier volume relative to 2020 remains between the years 2047 and 2100 (Fig. S7). When including glaciers that completely disappear by the end of the century, differences between volume projections get small. Therefore, to assess the differences due to the model options, we focused only on the subset of glaciers that still exist in 2100 for the subsequent option comparison analysis.

4.1 How do volume projections from temperature-index model options differ?

For the Aletsch glacier, volume projections vary considerably between the temperature-index model options with differences of up to 24% in 2100, relative to the 2020 volume, under SSP1-2.6 (Fig. 5a). Over time, the MB model choice influence on the projections increases under SSP1-2.6 for Aletsch glacier (Fig. 5a) and other non-vanishing glaciers (Fig. 6b–e), as nonlinear feedbacks start to contribute more than the pure climate change signal.

Temperature lapse rate choice

The temperature lapse rate choice has the most systematic influence on glacier projections with smaller glacier volumes in 2100 for the variable (and less negative) temperature lapse rates compared to the constant option (Fig. 6b, similar for SSP5-8.5 in Fig. S8b). The elevation distribution of retreating glaciers is located at higher elevations compared to the calibration period (i.e., 2000-2019). Thus, the smaller calibrated degree-day factor cannot compensate any more for the increasing influence of the less negative temperature lapse rate and the stronger glacier mass loss for the variable (less negative) temperature lapse rate option increases when the glacier retreats further.

Surface-type distinction choice

Applying a surface-type dependent degree-day factor instead of a constant degree-day factor results in a minimally smaller projected glacier in 2040, while for many glaciers it results in a relatively larger glacier volume in 2100 under SSP1-2.6 (stronger effect with linear compared to neg. exp. degree-day factor change, Fig. 6c, e). However, under SSP5-8.5, applying surface-type distinction results in both 2040 and 2100 in a smaller glacier compared to no surface-type distinction (Fig. S8c, e).

The explanation for the surface-type distinction dependent MB model differences in the case of the

SSP5-8.5 scenario and the first decades of SSP1-2.6 is likely that the glaciers' increased relative ice-covered ablation area plays a more critical role in future specific MB than during the calibration period. Thus, the CPDD are larger than in the calibration period, which results, as shown in the temperature sensitivity analysis of Fig. 4c, in higher negative specific MB anomalies when including surface-type distinction due to the higher ice degree-day factor (Fig. 2). However, in the last decades of SSP1-2.6, many glaciers are projected to retreat enough to get into a quasi-equilibrium state or even advance again slightly because of local cooling (e.g. Aletsch glacier in Fig. 5a). This effect cannot be explained by the fixed-geometry temperature sensitivity experiment of Fig. 4. Only when considering the glacier retreat does the accumulation area ratio increase so that the smaller snow degree-day factor becomes more important than the calibration period and can thus explain the larger glacier volumes.

Temporal climate resolution choice

Using pseudo-daily or daily instead of monthly temperature data results in either smaller or larger future projected glacier volumes with a more extensive spread under the daily option (Fig. 6d, f). In the pseudo-daily option, only the melt component can be different to the monthly option (if using the same precipitation factor). Either melt increases if the influence of the monthly melt threshold is larger than the influence from the smaller calibrated degree-day factor applied in the pseudo-daily option (Fig. 4) or vice-versa.

The melt component of the daily option is likely influenced by an additional aspect, the changing daily temperature standard deviation with increasing temperatures. The possible reason is that GCMs predict decreasing standard deviations over time, which decrease the melt threshold influence and thus increase the influence of the likewise smaller calibrated degree-day factor (see Fig. S9 for details).

Another difference in the daily option is the daily liquid or solid precipitation. In a warmer climate, under the same precipitation, both winter accumulation and summer ablation might decrease for the daily MB model due to decreased solid winter precipitation and a decreased melt threshold influence (also visible in the MB climate sensitivity analysis of Fig. 4a). In essence, projected differences between daily and monthly options depend on whether and how the balance shifts between the calibrated parameter differences and the influence of thresholds for melt and solid precipitation.

4.2 How do volume projections from the calibration choice options differ?

In the first decades, the five calibration choice options influence the Aletsch glacier volume projections more than the MB model choice (Fig. 5). For calibration options with a relatively small precipitation factor (C_1, C_2, C_5; all with very similar MB model parameters), the Aletsch glacier is projected to lose less volume in the first decades but more in the last 40 years of the 21st century compared to the options with a larger precipitation factor. For SSP1-2.6, Aletsch glacier could retreat to higher altitudes where it survives and even grows as the increased precipitation (of which more is solid at higher altitudes) outweighs the larger degree-day factor for that calibration option. The same is valid for other glaciers (e.g., the Hintereisferner glacier in Fig. S7).

For all non-vanishing analysed glaciers (Fig. 6g), the different calibration options result in similar projected individual glacier volumes in 2040, but their estimates diverge in 2100. With additional glacier-specific data, such as using the average winter MB or standard deviation of the annual MB to calibrate the MB model parameters (i.e., done in C_1, C_2, C_3), slightly more glacier volume is projected to be lost under SSP1-2.6. This effect gets stronger under SSP5-8.5 for the 15 remaining glaciers (Fig. S8g). However, the calibration option's influence on the glacier projections depends strongly on the individual glacier. Possible reasons are which calibration options use a relatively larger precipitation and degree-day factor, and whether the glacier is more in an ablation- or accumulation-dominant situation than during the calibration period. Additionally, the MB model choices' influence on volume projections differs between the calibration options. Generally, using more data for calibration and allowing for glacier-specific MB model parameters (i.e., C_1) creates a more extensive spread between the MB model options than using less observational data (smallest spread for C_4), which increases over time (Fig. S10).

5 DISCUSSION

5.1 Temperature-index model parameter choice differences

We analyse how our MB model parameter distributions differ to other studies. The range of the degree-day factor of ice in this study for MB model options with surface-type distinction (Fig. 2) is within the applied range of other local and regional temperature-index models (e.g. Rounce and others, 2020b; Huss and Hock, 2015; Braithwaite, 2008). Note that the unit of the degree-day factor in e.g. Huss and Hock (2015); Braithwaite (2008) is in mm K^{-1} day^{-1}, however, they actually mean mm w.e. K^{-1} day^{-1}.

Our average precipitation factor, considering all model and calibration options, is around three (Fig. 2), which is higher than previous studies (e.g. in Huss and Hock, 2015; Rounce and others, 2020b). The higher precipitation factor is likely due to differences in the climate datasets, glaciers investigated, precipitation gradients, and/or calibration schemes. For example, Huss and Hock (2015); Zekollari and others (2019) restrict the precipitation factor to a maximum value of two and proceed to change the degree-day factor or temperature bias accordingly to match observations.

The overparameterisation issue results in different combinations of the three MB model parameter combinations matching equally well when only one observation is available. Higher degree-day factors can be balanced by larger precipitation factors or lower temperature biases (Fig. 1a, b, equally found in Rounce and others, 2020b). Consequently, many factors besides the MB model choices determine the calibrated MB model parameters, which complicates comparisons.

5.2 Fixed-geometry model differences

Our study showed that different MB model or calibration options can result in considerable differences in modelled interannual, seasonal and elevation-dependent MB (Fig. 1, Fig. S4, Fig. 3) even over the calibration period. Here we discuss whether more complex MB models improve projections, how sensitive different MB models are to the climate and the added value of more observations.

MB model performance comparisons

Our goal was to determine the best temperature-index model option for a calibration option where just geodetic glacier observations are available (here C_5). While different MB model option combinations can have a similar performance as different aspects balance each other out (Fig. 3a, Fig. S5), using daily data, variable (less negative) lapse rates and a varying neg. exp. degree-day factor is arguably the most realistic physically, and matches the MB profile best under option C_5 (Fig. 3a, Fig. S5b). Furthermore, this combination could be calibrated and applied for 235 out of 247 glaciers with option C_5 (3rd best combination, Fig. S3b). The other MB model options could be used for 213 (monthly, constant & linear degree-day factor change) to 240 (pseudo-daily, variable, & no degree-day factor change) glaciers. To our knowledge, this is the first study that compares the performance of variations of temperature-index models and evaluates the use of daily climate data at regional scales.

Several studies compared temperature-index models to more complex MB models with a separate shortwave radiation term. These enhanced temperature-index models seem to perform better by reducing the sensitivity of the temperature-index models to temperature changes (Gabbi and others, 2014), although another study found no difference in performance over short time periods (Réveillet and others, 2017). In a regional-scale study, Huss and Hock (2015) did not find an added value in model performance when using the even more complex, simplified energy-balance model of Oerlemans (2001) instead of their temperature-index model.

The lack of calibration and validation data at regional and global scales makes it difficult to assess the added value of model complexity. Using more complex temperature-index or energy-balance models usually requires more glacier-specific free parameters, and fixing them on a regional level may overshadow uncertainties from overparameterisation.

MB model climate sensitivity differences

We compare our climate sensitivities to similar experiments by Bolibar and others (2022, all 660 French Alpine glaciers) and Vincent and Thibert (in review, 2 Alpine glaciers). Bolibar and others (2020) found that using a deep learning MB model with daily temperature, precipitation, snowfall, and glacier topography as input to model annual MB outperformed a linear LASSO (i.e., a regularised multi-linear regression) model in a case study of 32 glaciers in the French Alps, specifically for extreme MB. However, their LASSO MB model behaves differently than a temperature-index model, and it is unclear how different temperature-index model options would behave in comparison. We therefore designed a similar experiment with our temperature-index model options (Fig. 4).

Without surface-type dependent degree-day factor change, our models respond to CPDD anomalies in a similar fashion to the LASSO MB model of Bolibar and others (2022). Our study found nonlinear MB responses to CPDD anomalies when including surface-type distinction (Fig. 4b). It was not possible to analyse very negative CPDD anomalies as CPDD is defined as positive. This increased sensitivity with increasing CPDD was qualitatively also found in Vincent and Thibert (in review) using a temperature-index model with separate degree-day factors for snow and ice. The deep-learning MB model of Bolibar and others (2022) captured a similar but less pronounced nonlinearity. A part of the physical explanation for the nonlinearities found in all three studies could be that for large positive CPDD anomalies, snow on the surface is lost, and thus a greater fraction of the glacier's surface is ice, which is more temperature-sensitive. The less pronounced nonlinearity in Bolibar and others (2022) hints at other counteracting processes detected by the deep-learning MB model (e.g. possible decreasing MB sensitivity with increasing temperatures due to reduced solar radiation importance in a warming world). Also, CPDD anomalies in Bolibar and others (2022) were only distributed over the ablation season, and surface-type distinction was only modelled implicitly by the neural network.

Our study found a driver-dependent specific MB sensitivity for solid winter and summer precipitation anomalies. If induced by temperature changes, solid winter or summer precipitation anomalies create non-linearities with either increasing or decreasing MB sensitivity to changes in solid precipitation (Fig. 4d, e) for all of our MB model options. On the other hand, precipitation-induced solid winter or summer precipitation anomalies were linearly related to the specific MB for MB models without surface-type distinction and nonlinear, with increasing negative specific MB, for MB models with surface-type distinction (Fig. 4g, h).

In Vincent and Thibert (in review), the MB sensitivity to their precipitation-induced solid winter precipitation anomalies increases for negative anomalies, i.e., qualitatively similar to our experiment when accounting for surface-type dependent degree-day factors (Fig. 4g). Bolibar and others (2022) directly use solid winter or summer precipitation anomalies as predictors in their MB models. Consequently, in their study, solid winter precipitation anomalies are independent of temperature changes and solid summer precipitation, and vice-versa. Our precipitation-induced solid precipitation anomaly is, therefore, similar to the experiments in Bolibar and others (2022), although in our case, solid winter and summer precipitation are linearly correlated by the applied precipitation factor that modifies the annual precipitation.

Similar to our MB models without surface-type distinction, the LASSO MB model of Bolibar and others (2022) results in a linear relation between precipitation-induced solid precipitation and MB. However, unlike all our MB model options, the deep learning MB model of Bolibar and others (2022) has a larger MB sensitivity for small solid precipitation anomalies and a smaller MB sensitivity for strong positive and negative anomalies, specifically for solid summer precipitation anomalies. Different induced correlations make it complex to compare the experiments between the studies. Although the applied solid precipitation anomalies in Bolibar and others (2022) were independent of other variables such as temperature, the deep-learning MB model was trained with data where e.g. positive solid summer precipitation anomalies were related to negative temperature anomalies. The reason is that over the historical (and future) climate, climatological solid precipitation anomalies induced by temperature changes are more common than precipitation changes. The decreasing MB sensitivity for positive solid summer precipitation anomalies in Bolibar and others (2022) was equally found for all of our MB model options if applying a temperature-induced solid summer precipitation anomaly. The opposing nonlinear sensitivities for negative anomalies remain to be explained. Bolibar and others (2022) argue that the deep-learning MB model might capture decreasing ice degree-day factors for increasing temperatures (Braithwaite, 1995; Huss and others, 2009). An explanation for that would be a temporally changing relation between melt and temperature due to non-changing shortwave radiation fluxes but changing longwave radiation and turbulent fluxes (Gabbi and others, 2014; Ismail and others, 2023). These processes are not implemented in our models, and further study is necessary to test this hypothesis.

To better understand different MB model sensitivities, it would be necessary to directly compare our model variants to models separating shortwave radiation from temperature-induced melt (e.g. enhanced temperature-index or energy-balance models, Gabbi and others, 2014). Theoretically, if incoming shortwave radiation stays constant, the MB model temperature sensitivity would decrease for more positive CPDD anomalies with these enhanced MB models (Ismail and others, 2023). The nonlinearity of decreased shortwave radiation importance can counteract those from models with surface-type distinction. Depending on which feedback is critical, a MB model without surface-type distinction could, by chance, behave more similarly to one with both surface-type distinction and a separate shortwave radiation term. However, model parameter calibration might strongly influence the outcome, and the effect of overparameterisation should be analysed. Another feedback is the changing hypsometry, which we and the other two studies did not include in the sensitivity experiment (further discussed in Sect. 4.1, 5.3).

Added value of additional observational data for the calibration

We found a slightly improved MB model performance for calibration options with more observational data, specifically when using the interannual MB variability to calibrate the precipitation factor for every glacier (Fig. 3b, Fig. S6). The climate dataset choice can have a similar influence on the model performance as the precipitation factor choice, i.e., both a climate dataset with larger winter precipitation (Compagno and others, 2021) or a larger precipitation factor (Fig. 1e) result in a larger winter MB.

Using 16 regionally fixed parameter sets of precipitation factors and degree-day factors and only changing the temperature bias on a glacier-per-glacier level resulted in poorer model performance for Huss and Hock (2015) compared to their reference parameter calibration option for glaciers in the European Alps. Their reference parameter calibration option was a three-step calibration scheme varying first the precipitation factor in a specific range, then, if necessary, the degree-day factor within a range, followed by the temperature bias.

When optimising six MB model parameters to geodetic, point stake data and transient snowline retreat, the resulting parameter combination ensemble showed only little spread over historical MB estimates on a single glacier in Geck and others (2021). Their small overparameterisation influence likely results from both higher temporally and spatially resolved MB observations for calibration and smaller downscaling parameter ranges since weather station data was used to force their enhanced temperature-index model.

We found that in-situ glacier MB observations could improve the model performance and reduce uncertainties due to overparameterisation. Thus, potential future remote sensing data on regional to global scales to estimate the MB gradient, seasonal and interannual MB will improve model performance by better constraining free model parameters. Interferometric swath altimetry applied on CryoSat-2 produces seasonal and multiannual glacier thinning estimates at unprecedented monthly temporal resolution (Jakob and others, 2021), yet at coarse spatial resolution (100x100 km bins). By combining glacier thinning with surface velocity observations and ice thickness estimates, altitudinally-resolved specific mass balances can be derived (Miles and others, 2021). Those are, however, uncertain, specifically over the accumulation period, as each of the necessary variables is uncertain. Additionally, these new techniques and datasets are not yet globally available and need to convert elevation to mass changes which results in further uncertainties that are in total much larger than in-situ observations (Huss, 2013), i.e., firn densification models might be needed to reduce these uncertainties. Using higher-resolved dynamically downscaled climate data could also constrain the local downscaling parameter range (e.g. Karger and others, 2017). It is however unlikely that large-scale studies will benefit from drastically improved forcing data in the near future. Here, glacier models combined with remote sensing could even help to detect forcing biases (e.g. Guidicelli and others, 2022).

Without this additional remote-sensing data, we favour calibration option C_5 over C_4 for OGGM users. Using glacier-specific precipitation factors depending on the glaciers' average winter precipitation (C_5) instead of the same precipitation factor for every glacier (C_4) results in a less wide distribution, i.e., unrealistically large precipitation values that occur for C_4 are avoided (Fig. S1b). In C_5, we use the logarithmic relation between winter precipitation and calibrated precipitation factor of option C_2, where winter MB is matched. Thus another reason to use C_5 is that the precipitation factor dependence on the winter precipitation could make physically more sense and is independent of the model choice. The precipitation factor depends rather on winter MB than interannual variability as winter MB depends mostly on the amount of solid precipitation, and most precipitation is solid in winter (at least in mid- and high-latitude climates).

5.3 Dynamic volume and runoff projection differences

We projected that Aletsch glacier, the largest glacier in the European Alps, loses 50-83% of its volume under SSP1-2.6, and $> 95\%$ under SSP5-8.5, relative to 2020, for the different MB model and calibration options of this study (Fig. 5). Aletsch glacier projections from a full-stokes glacier model (Jouvet and others, 2011) and two dynamical large-scale glacier model studies (Rounce and others, 2023; Zekollari and others, 2019) under approximately the same climate scenarios lie at the lower part of our loss ranges. The reasons for these differences are difficult to disentangle. In the sections below, we compare our results with previous studies and analyse the influence of model choice on projections of glacier runoff, one of the most important variables for future planning.

MB model influence on volume projections

In a warming climate, less negative temperature lapse rates result in more projected glacier loss (Fig. 6, lapse-rate option "variable"). How different our lapse rates are from other large-scale glacier studies (Huss and Hock, 2015; Zekollari and others, 2019; Rounce and others, 2020a) is unknown. It also needs to be clarified how well the ERA5-derived free-atmosphere temperature lapse rates used here and in these studies are related to near-surface temperature lapse rates. Some studies suggest that the near glacier-surface lapse rates are rather weaker during the ablation season compared to the free-atmosphere estimates (e.g. Gardner and others, 2009; Hodgkins and others, 2013). Our ERA5-derived estimates are, however, stronger (more negative) in the ablation compared to the accumulation season (not shown).

Interestingly, the temporal climate resolution choice has no systematic influence on regional glacier change projections (Fig. 6d, f). Using the pseudo-daily climate option with no future changes in the daily temperature standard deviation, i.e., as applied in Huss and Hock (2015) and Zekollari and others (2019), results only in minor projection differences compared to the monthly climate option. The influence of using daily instead of monthly data depends on how the balance shifts between calibrated parameter differences and the impact of thresholds for melt and solid precipitation. However, when coupling glacier models with hydrological models, it can be beneficial to use daily climate data to get daily runoff output data.

The response of MB models with and without surface-type distinction (Fig. 6, Fig. S8) depends on the

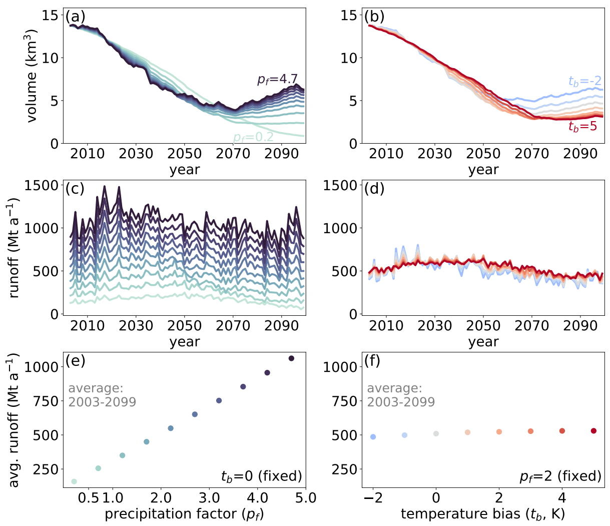

Fig. 7. Influence of downscaling MB model parameters on **(a, b)** volume and **(c, d)** runoff projections for the Aletsch glacier, European Alps, using the reference temperature-index model during the period 2003-2099. The colors indicate the chosen precipitation factor (p_f) or temperature bias (t_b) as presented in **(e, f)**, which shows the relation between model parameter and average annual runoff. On the left plots, **(a, c, e)**, t_b is set to zero and p_f is varied while on the right plots, **(b, d, f)**, p_f is set to 2 and t_b is varied. Although all parameter combination choices are calibrated to the same average geodetic MB, they differ substantially in volume and runoff estimates. Future projections are the median estimates from five GCMs under the SSP1-2.6 scenario. The four different runoff components from OGGM are in Fig. S11. Fig. S12 shows the same for the Hintereisferner glacier.

future glacier state. If the future accumulation area ratio is smaller than during the calibration period, MB models with surface-type distinction cause more mass loss (more melt over ice), and vice versa for larger accumulation area ratios (less melt over snow).

Other large-scale glacier models did not analyse the influence of the small temperature-index model changes as we did in our study. When comparing their temperature-index model to a simplified energy-balance model, Huss and Hock (2015) found that the energy-balance model reduced glacier loss projections by about 20%, which is in the same order of magnitude as the projection differences from our temperature lapse rate options.

Calibration option and overparameterisation influence on volume projections

We found slightly more glacier volume loss when calibrating glaciers with additional in-situ observations (Fig. 6). The differences vary on an individual glacier level, e.g., on the precipitation versus degree-day factor choice (exemplarily shown in Fig. 7a, b) and the accumulation-area ratio relative to the calibration period. These differences also show the influence of overparameterisation on glacier volume projections, as all options equally match the one geodetic observation. For the Aletsch glacier, a larger precipitation factor results in a faster projected mass loss in the first decades but causes less projected mass loss at the end of the century under SSP1-2.6 (Fig. 7a).

In Huss and Hock (2015), overparameterisation influenced glacier projections of selected regions by ±18% compared to their reference calibration option (assessed by 16 fixed parameter combinations). Compagno and others (2021) analysed the influence of small precipitation factor range shifts (±0.6) in their three-step calibration and found glacier projection differences of ⩽4%. A larger precipitation factor range and a different order in their three-step calibration could result in more significant differences. Rounce and others (2020a) found that glacier volume projections can be greatly affected by overparameterisation at the glacier scale but are much less affected by overparameterisation compared to the GCM choice at the regional scale. However, the influence might depend on their method for aggregating uncertainties at the regional scale. Furthermore, they argue that other metrics, such as glacier runoff projections, are more systematically influenced by the MB model parameter choice.

Fixed-gauge glacier runoff projection differences

Besides examining differences in glacier volume changes, we repeated our comparisons for fixed-gauge glacier runoff (here the sum of the melt and liquid precipitation components from the formerly glacierized area) changes (Fig. 7, Fig. S11–17). We found that the MB model options considerably systematically influence glacier runoff projections (Fig. S13a, Fig. S15a, Fig. S17a). In many cases, using variable (less negative) lapse rates, daily climate resolution, and no surface-type distinction resulted in larger annual runoff (Fig. S17b–f). We found a strong annual glacier runoff increase for larger precipitation factors (exemplarily shown in Fig. 7c, e), while the temperature bias choice has only minimal non-systematic influence (Fig. 7d, f). A larger precipitation factor directly increases the liquid precipitation and also indirectly increases the melt runoff components due to a larger calibrated degree-day factor (Fig.1a, Fig. S11). If different precipitation factors are used, glacier runoff varies strongly between the calibration options (e.g. Fig. S13b for Aletsch glacier) and is smallest for the calibration option with the overall smallest precipitation factor (i.e., C_4, Fig. 2, Fig. S17g for 83 examined glaciers). How and if total runoff is influenced by the temperature bias depends on the runoff components allocation and their temperature influence. For the Aletsch glacier, the runoff components compensate for one another over the entire period (Fig. 7d, f).

Studies suggest that interannual precipitation might influence glacier runoff less than temperature changes (e.g. Banerjee and others, 2022; Pramanik and others, 2018). The reason is that larger annual precipitation can result in similar annual glacier runoff, as decreased melt runoff compensates for increased liquid precipitation. This does not contradict our reversed relation found for the climate downscaling model parameters (Fig. 7e, f), as we vary the precipitation factor or temperature bias before the calibration. Thus, the degree-day factor changes as well (see Fig. 1a, b) and influences the melt runoff components (Fig. S11a, b). Therefore, different model parameter combinations influence the runoff in a different way compared to changing climate patterns of temperature and precipitation.

Comparisons to GlacierMIP2 and Rounce and others (2023)

GlacierMIP2 (Marzeion and others, 2020) compared projections of different large-scale glacier models in a coordinated effort. The sources of the projection differences were difficult to disentangle as not only the MB model but also the calibration strategy, climate data, and the initial state were different between glacier models. The study also estimated each model's sensitivity of the mean specific mass balance to temperature changes using an inverse approach which we repeated with our MB model variants. We found a lower negative temperature sensitivity when not including surface-type distinction or using daily instead of monthly data (not shown). Similarly, in GlacierMIP2, from the four near-global models using temperature-index models, those without surface-type distinction (Maussion and others, 2019; Marzeion and others, 2012) had a lower negative temperature sensitivity than those with different degree-day factors between surface types (Huss and Hock, 2015; Radić and others, 2014). However, besides the MB model option specifics analysed in our study, the applied local-scale climate, dependent on, e.g., the chosen precipitation factor, climate datasets, or precipitation gradients, also influences the temperature sensitivity differences. One of the two energy-balance models from GlacierMIP2 had the lowest temperature sensitivity (Shannon and others, 2019). Both energy-balance models generally projected the least negative mass balances. The reason might be relatively small future changes in downwelling long- and short-wave radiation despite increasing temperatures (Shannon and others, 2019) and thus a possible temperature-oversensitivity of temperature-index models (see Sect. 5.2). Nonetheless, the influence of overparameterisation on large-scale energy-balance model projections needs to be better determined.

The model used to create projections for Rounce and others (2023) is most similar to OGGM as it uses the glacier dynamics module of OGGM, but the MB module of the Python Glacier Evolution model (PyGEM). Rounce and others (2023) project in 2100 around 16% lower relative glacier volume than our median projections under SSP1-2.6 (for all model options, three common GCMs, and 41 non-vanishing glaciers). The differences are reduced on median to 2-15% lower relative glacier volumes (calibration option dependent) when comparing only to our temperature-index model that resembles most to Rounce and others (2023) (i.e., variable lapse rates, neg. exp. degree-day factor change and pseudo-daily climate). Specifically, applying the same temperature lapse rate approach reduced the volume projection differences. The absolute runoff projections of Rounce and others (2023) are generally smaller and the runoff got reduced stronger from 2020 until 2100 compared to our options (using 85 common examined glaciers). These volume and runoff projection differences that increase on an individual-glacier level might result from the study-specific choices in the parameter calibration, bias correction, and temperature-index model.

5.4 Limitations

Due to the lack of robust, high temporally and spatially resolved observational data, we only analysed 88 glaciers, of which most come from the northern mid-latitudes (28 from Central Europe and 19 from Scandinavia). Around half of these glaciers vanish by 2100 for at least one of the options, even under SSP1-2.6. The examined sample may thus not represent the response of global glacier mass. In addition, some glaciers could not be calibrated with the proposed calibration options, hinting at missing model physics, poorly downscaled local climate, or MB observational errors.

Although higher-resolved geodetic estimates exist regionally (e.g. Miles and others, 2021; Jakob and others, 2021), we only used the more robust in-situ and 20-year average geodetic MB observations. We neglected uncertainties from all used MB observations. The observation uncertainties and overparameterisation could be estimated using Bayesian inference (Rounce and others, 2020b). However, it remains challenging to aggregate and disentangle these uncertainties from individual to regional scales. We also did not assess the influence of uncertainties from GCMs, which can be larger than uncertainties from over-parameterisation (e.g. Rounce and others, 2020a). Initial state and bias correction uncertainties are also neglected. Instead, we focused on the temperature-index model design and MB model calibration choice.

As small changes in the temperature-index model already had such an influence, we did not implement more enhanced MB models, which could be the next step. However, even simple choices such as how the degree-day factor gradually changes with ageing snow still need to be determined. We propose two approximations but believe that the neg. exp. degree-day factor change option is more appropriate than the linear option. We could also have applied more simple surface-type distinction methods with a step-wise change between snow, firn and ice (e.g. Huss and Hock, 2015; Rounce and others, 2020a). We chose the monthly ageing snow ageing bucket system (see Sect. A.1), as this scheme could eventually be used to estimate firn densification and thus calibrate on more robust elevation changes instead of MB with an assumed density conversion. We did not explicitly include refreezing, as large-scale observations, e.g. englacial temperature, are missing; nor did we include debris cover.

We vary three MB model parameters and keep them constant over time, although e.g. the snow degree-day factor was found to vary specifically under clear-sky conditions (e.g., depending on altitude and solar inclination) and changing cloud cover creates temporal instability of the parameter (Ismail and others, 2023). In addition, the influence of using daily or monthly climate data could equally depend on the chosen solid precipitation and melt thresholds which we fixed to global values. For example, Matthews and Hodgkins (2016) found that tuning the melt threshold increased their skill and resulted in a more stationary degree-day factor over their 34-year study period. Furthermore, we assume constant temperature lapse rates and the choice of lapse rate strongly influenced the MB. Due to the lack of data, we neglect changes in the temperature lapse rate in the future, such as enhanced warming rates with elevation (Pepin and others, 2015; Palazzi and others, 2019), so we might underestimate glacier mass loss.

We did not include glacier hypsometry changes for the (non)linear climate sensitivity analysis of Sect. 3.5. Thus, these theoretical sensitivities differed from our dynamical projection findings where glaciers can adapt to the changing climate. For the calibration over the 20 years, we also do not apply ice dynamics, i.e., the glacier area is fixed. This assumption can result in mass change overestimates, specifically for glaciers with higher mass flux rates (Mukherjee and others, 2022).

6 CONCLUSIONS

Our findings suggest that often considered small model design changes, such as variations of temperature-index models and calibration options, can influence performance as well as volume and runoff projections. By changing only one model option at a time within the OGGM framework, we provide insight into glacier model behaviour differences that are impossible in large-scale glacier model intercomparison projects.

During the calibration period, due to overparameterisation, even the simplest temperature-index model responded differently to different combinations of fixed MB model parameters, although all models matched the average geodetic MB. For example, we found increasing interannual MB variability, winter MB and MB elevation gradients for increasing precipitation factors and decreasing temperature biases. To assess the added value of a given process and, simultaneously, of better-resolved MB observations, we focussed on 88 glaciers with available in-situ observations. While specifically using the interannual MB variability to calibrate otherwise fixed parameters led to better MB model performance (i.e., average modelled MB profile coincided better with observations), the added value of additional MB complexity is challenging to demonstrate. Nevertheless, performance was among the best for the most physically realistic MB model option combination with surface-type distinction with a negative exponential degree-day factor change, variable lapse rates and daily data. Matching approximately the observed MB gradient is essential as it directly influences the ice flux and, therefore, the assumed ice dynamics (Farinotti and others, 2009; Maussion and others, 2019). Without additional available calibration data, choosing the precipitation factor dependent on the glacier's winter precipitation might make physically more sense than a globally fixed precipitation factor, although we could not find an added value in the MB model performance. Over a fixed glacier geometry, temperature-induced solid precipitation anomalies created nonlinear sensitivities to the specific MB for all examined temperature-index models. In contrast, cumulative positive-degree-day anomalies responded only nonlinear for models with included surface-type distinction.

For projections that included ice dynamics and hypsometry feedback to allow glaciers to retreat to higher altitudes, the MB models responded strongly nonlinearly. The influence of a specific MB model choice depended on the differences between the future glacier state and climate compared to the calibration period. These patterns were consistent over the various calibration and other MB model options; thus, the projection differences between temperature-index models were also a result of their design differences and did not solely stem from overparameterisation. In a warmer climate, less negative temperature lapse rates resulted in systematically smaller projected glaciers by 2100. In addition, using monthly-changing snow-age dependent degree-day factors produced more or less glacier loss depending on whether the glacier accumulation area ratio is smaller or larger than during the calibration period. For example, under SSP1-2.6, the still existing examined glaciers resulted in smaller volumes in the first decades when including the surface-type distinction, while in the long term, it mainly resulted in larger volumes. Also, applying daily instead of monthly climate data can result in a larger or smaller glacier in a warmer climate. The outcome depended on how the balance shifts between the thresholds (melt and solid precipitation) and the correspondingly different calibrated model parameters. With more data in the calibration, glacier volume projections got smaller overall. However, at the scale of individual glaciers, the influence went both ways, partly illustrating the overparameterisation uncertainties.

Comparisons between options were difficult, as we projected that half of the examined glaciers with in-situ data will lose 50% of their volume by 2039, relative to 2020, independent of the climate scenario. As we showed that additional observations have the potential to reduce projection uncertainties, it is necessary to search for more climate-resilient glaciers to continue long-term in-situ observations and for better-resolved remote large-scale glacier-specific MB observations. While glacier model designs of, e.g. GlacierMIP2 differed much more than our model options, we found that even small changes, such as the temperature-index model design or calibration choice, can substantially influence individual glacier projections. That influence can increase over time for the non-vanishing glaciers and becomes even more important when considering direct adaptation-critical estimates such as glacier runoff changes. These findings thus advance our understanding of projected uncertainties and the differences between glacier models and may be used to make informed decisions with respect to the MB model and calibration options.

7 CODE AND DATA AVAILABILITY

The code to create the figures is publicly available in the Github repository `https://github.com/lilianschuster/oggm_mb_sandbox_option_intercomparison` that used the OGGM massbalance-sandbox repository (`https://github.com/OGGM/massbalance-sandbox`). The projections and other data are publicly available via Zenodo: `https://doi.org/10.5281/zenodo.7660887`.

8 ACKNOWLEDGEMENTS

The authors would like to thank Jordi Bolibar for the useful discussions on the MB model climate sensitivities (Sect. 3.5, 5.2). Lilian Schuster is recipient of a DOC Fellowship of the Austrian Academy of Sciences at the Department of Atmospheric and Cryospheric Sciences, University of Innsbruck (No. 25928). She has also been funded by University of Innsbruck's "Exzellenzstipendien für Doktoratskollegs" fellowship programme. This project has received additional funding from the European Union's Horizon 2020 research and innovation programme under grant agreement No. 101003687. This text reflects only the author's view and that the Agency is not responsible for any use that may be made of the information it contains. This project was also supported by NASA under grant Nos. 80NSSC20K1296 and 80NSSC20K1595.

9 SUPPLEMENTARY MATERIAL

The supplementary material for this article can be found at [TODO: LINK].

REFERENCES

Anderson B and Mackintosh A (2012) Controls on mass balance sensitivity of maritime glaciers in the Southern Alps, New Zealand: The role of debris cover. *Journal of Geophysical Research: Earth Surface*, **117**(F01003) (doi: 10.1029/2011JF002064)

Banerjee A, Singh U and Sheth C (2022) Disaggregating geodetic glacier mass balance to annual scale using remote-sensing proxies. *Journal of Glaciology*, 1–10 (doi: 10.1017/jog.2022.89)

Bolibar J, Rabatel A, Gouttevin I, Galiez C, Condom T and Sauquet E (2020) Deep learning applied to glacier evolution modelling. *Cryosphere*, **14**(2), 565–584 (doi: 10.5194/tc-14-565-2020)

Bolibar J, Rabatel A, Gouttevin I, Zekollari H and Galiez C (2022) Nonlinear sensitivity of glacier mass balance to future climate change unveiled by deep learning. *Nature Communications*, **13**(1), 409 (doi: 10.1038/s41467-022-28033-0)

Braithwaite RJ (1995) Positive degree-day factors for ablation on the Greenland ice sheet studied by energy-balance modelling. *Journal of Glaciology*, **41**(137), 153–160 (doi: 10.3189/S0022143000017846)

Braithwaite RJ (2008) Temperature and precipitation climate at the equilibrium-line altitude of glaciers expressed by the degree-day factor for melting snow. *Journal of Glaciology*, **54**(186), 437–444 (doi: 10.3189/002214308785836968)

Braithwaite RJ and Olesen OB (1989) Calculation of Glacier Ablation from Air Temperature, West Greenland. In J Oerlemans (ed.), *Glacier Fluctuations and Climatic Change*, 219–233, Springer Netherlands, Dordrecht, ISBN 978-94-015-7823-3 (doi: 10.1007/978-94-015-7823-3{_}15)

Church J, Clark P, Cazenave A, Gregory J, Jevrejeva S, Levermann A, Merrifield M, Milne G, Nerem R, Nunn P, Payne A, Pfeffer W, Stammer D and Unnikrishnan A (2013) Sea Level Change. In Intergovernmental Panel on Climate Change (ed.), *Climate Change 2013 - The Physical Science Basis*, chapter 13, 1137–1216, Cambridge University Press, Cambridge (doi: 10.1017/CBO9781107415324.026)

Compagno L, Zekollari H, Huss M and Farinotti D (2021) Limited impact of climate forcing products on future glacier evolution in Scandinavia and Iceland. *Journal of Glaciology*, **67**(264), 727–743 (doi: 10.1017/jog.2021.24)

Compagno L, Huss M, Miles ES, McCarthy MJ, Zekollari H, Dehecq A, Pellicciotti F and Farinotti D (2022) Modelling supraglacial debris-cover evolution from the single-glacier to the regional scale: an application to high mountain asia. *The Cryosphere*, **16**(5), 1697–1718 (doi: 10.5194/tc-16-1697-2022)

Edwards TL, Nowicki S, Marzeion B, Hock R, Goelzer H, Seroussi H, Jourdain NC, Slater DA, Turner FE, Smith CJ, McKenna CM, Simon E, Abe-Ouchi A, Gregory JM, Larour E, Lipscomb WH, Payne AJ, Shepherd A, Agosta C, Alexander P, Albrecht T, Anderson B, Asay-Davis X, Aschwanden A, Barthel A, Bliss A, Calov R, Chambers C, Champollion N, Choi Y, Cullather R, Cuzzone J, Dumas C, Felikson D, Fettweis X, Fujita K, Galton-Fenzi BK, Gladstone R, Golledge NR, Greve R, Hattermann T, Hoffman MJ, Humbert A, Huss M, Huybrechts P, Immerzeel W, Kleiner T, Kraaijenbrink P, Le clec'h S, Lee V, Leguy GR, Little CM, Lowry DP, Malles JH, Martin DF, Maussion F, Morlighem M, O'Neill JF, Nias I, Pattyn F, Pelle T, Price SF, Quiquet A, Radić V, Reese R, Rounce DR, Rückamp M, Sakai A, Shafer C, Schlegel NJ, Shannon S, Smith RS, Straneo F, Sun S, Tarasov L, Trusel LD, Van Breedam J, van de Wal R, van den Broeke M, Winkelmann R, Zekollari H, Zhao C, Zhang T and Zwinger T (2021) Projected land ice contributions to twenty-first-century sea level rise. *Nature*, **593**(7857), 74–82 (doi: 10.1038/s41586-021-03302-y)

Eyring V, Bony S, Meehl GA, Senior CA, Stevens B, Stouffer RJ and Taylor KE (2016) Overview of the Coupled Model Intercomparison Project Phase 6 (CMIP6) experimental design and organization. *Geoscientific Model Development*, **9**(5), 1937–1958 (doi: 10.5194/gmd-9-1937-2016)

Farinotti D, Huss M, Bauder A, Funk M and Truffer M (2009) A method to estimate the ice volume and ice-thickness distribution of alpine glaciers. *Journal of Glaciology*, **55**(191), 422–430 (doi: 10.3189/002214309788816759)

Farinotti D, Huss M, Fürst JJ, Landmann J, Machguth H, Maussion F and Pandit A (2019) A consensus estimate for the ice thickness distribution of all glaciers on Earth. *Nature Geoscience*, **12**(3), 168–173 (doi: 10.1038/s41561-019-0300-3)

Frederikse T, Landerer F, Caron L, Adhikari S, Parkes D, Humphrey VW, Dangendorf S, Hogarth P, Zanna L, Cheng L and Wu YH (2020) The causes of sea-level rise since 1900. *Nature*, **584**(7821), 393–397 (doi: 10.1038/s41586-020-2591-3)

Furian W, Maussion F and Schneider C (2022) Projected 21st-Century Glacial Lake Evolution in High Mountain Asia. *Frontiers in Earth Science*, **10**(March), 1–21 (doi: 10.3389/feart.2022.821798)

Gabbi J, Carenzo M, Pellicciotti F, Bauder A and Funk M (2014) A comparison of empirical and physically based glacier surface melt models for long-term simulations of glacier response. *Journal of Glaciology*, **60**(224), 1140–1154 (doi: 10.3189/2014JoG14J011)

Gangadharan N, Goosse H, Parkes D, Goelzer H, Maussion F and Marzeion B (2022) Process-based estimate of global-mean sea-level changes in the Common Era. *Earth System Dynamics*, **13**(4), 1417–1435 (doi: 10.5194/esd-13-1417-2022)

Gardner AS, Sharp MJ, Koerner RM, Labine C, Boon S, Marshall SJ, Burgess DO and Lewis D (2009) Near-surface temperature lapse rates over arctic glaciers and their implications for temperature downscaling. *Journal of Climate*, **22**(16), 4281–4298 (doi: 10.1175/2009JCLI2845.1)

Geck J, Hock R, Loso MG, Ostman J and Dial R (2021) Modeling the impacts of climate change on mass balance and discharge of Eklutna Glacier, Alaska, 1985-2019. *Journal of Glaciology*, **67**(265), 909–920 (doi: 10.1017/jog.2021.41)

Guidicelli M, Huss M, Gabella M and Salzmann N (2022) Snow accumulation over the world's glaciers (1981–2021) inferred from climate reanalyses and machine learning. *The Cryosphere Discussions*, **2022**, 1–47 (doi: 10.5194/tc-2022-69)

Hodgkins R, Carr S, Pálsson F, Guðmundsson S and Björnsson H (2013) Modelling variable glacier lapse rates using ERA-Interim reanalysis climatology: an evaluation at Vestari- Hagafellsjökull, Langjökull, Iceland. *International Journal of Climatology*, **33**(2), 410–421 (doi: 10.1002/joc.3440)

Hugonnet R, McNabb R, Berthier E, Menounos B, Nuth C, Girod L, Farinotti D, Huss M, Dussaillant I, Brun F and Kääb A (2021) Accelerated global glacier mass loss in the early twenty-first century. *Nature*, **592**(7856), 726–731 (doi: 10.1038/s41586-021-03436-z)

Huss M (2013) Density assumptions for converting geodetic glacier volume change to mass change. *The Cryosphere*, **7**(3), 877–887 (doi: 10.5194/tc-7-877-2013)

Huss M and Farinotti D (2012) Distributed ice thickness and volume of all glaciers around the globe. *Journal of Geophysical Research: Earth Surface*, **117**(4), F04010 (doi: 10.1029/2012JF002523)

Huss M and Hock R (2015) A new model for global glacier change and sea-level rise. *Frontiers in Earth Science*, **3**(September), 1–22 (doi: 10.3389/feart.2015.00054)

Huss M and Hock R (2018) Global-scale hydrological response to future glacier mass loss. *Nature Climate Change*, **8**(2), 135–140 (doi: 10.1038/s41558-017-0049-x)

Huss M, Funk M and Ohmura A (2009) Strong alpine glacier melt in the 1940s due to enhanced solar radiation. *Geophysical Research Letters*, **36**(23) (doi: 10.1029/2009GL040789)

IPCC (2021) *Climate Change 2021: The Physical Science Basis. Contribution of Working Group I to the Sixth Assessment Report of the Intergovernmental Panel on Climate Change.* edited by: Masson-Delmotte, V., Zhai, P., Pirani, A., Connors, S. L., Péan, C., Berger, S., Caud, N., Chen, Y., Goldfarb, L., Gomis, M. I., Huang, M., Leitzell, K., Lonnoy, E., Matthews, J. B. R., Maycock, T. K., Waterfield, T., Yelekçi, O., Yu, R., and Zhou, B., Cambridge University Press, Cambridge, United Kingdom and New York, NY, USA, In Press (doi: 10.1017/9781009157896)

Ismail MF, Bogacki W, Disse M, Schäfer M and Kirschbauer L (2023) Estimating degree-day factors of snow based on energy flux components. *The Cryosphere*, **17**(1), 211–231 (doi: 10.5194/tc-17-211-2023)

Jakob L, Gourmelen N, Ewart M and Plummer S (2021) Spatially and temporally resolved ice loss in High Mountain Asia and the Gulf of Alaska observed by CryoSat-2 swath altimetry between 2010 and 2019. *The Cryosphere*, **15**(4), 1845–1862 (doi: 10.5194/tc-15-1845-2021)

Jouvet G, Huss M, Funk M and Blatter H (2011) Modelling the retreat of Grosser Aletschgletscher, Switzerland, in a changing climate. *Journal of Glaciology*, **57**(206), 1033–1045 (doi: 10.3189/002214311798843359)

Karger DN, Conrad O, Böhner J, Kawohl T, Kreft H, Soria-Auza RW, Zimmermann NE, Linder HP and Kessler M (2017) Climatologies at high resolution for the earth's land surface areas. *Scientific data*, **4**(1), 1–20 (doi: 10.1038/sdata.2017.122)

Kaser G, Grosshauser M and Marzeion B (2010) Contribution potential of glaciers to water availability in different climate regimes. *P. Natl. Acad. Sci. Usa.*, **107**(47), 20223–20227 (doi: 10.1073/pnas.1008162107)

Klug C, Bollmann E, Galos SP, Nicholson L, Prinz R, Rieg L, Sailer R, Stötter J and Kaser G (2018) Geodetic reanalysis of annual glaciological mass balances (2001–2011) of Hintereisferner, Austria. *The Cryosphere*, **12**(3), 833–849 (doi: 10.5194/tc-12-833-2018)

Lange S (2019) Trend-preserving bias adjustment and statistical downscaling with ISIMIP3BASD (v1.0). *Geoscientific Model Development*, **12**(7), 3055–3070 (doi: 10.5194/gmd-12-3055-2019)

Lange S (2022) ISIMIP3BASD (doi: 10.5281/zenodo.7151476)

Lange S, Menz C, Gleixner S, Cucchi M, Weedon GP, Amici A, Bellouin N, Schmied HM, Hersbach H, Buontempo C and Cagnazzo C (2021) WFDE5 over land merged with ERA5 over the ocean (W5E5 v2.0) (doi: 10.48364/ISIMIP.342217)

Li F, Maussion F, Wu G, Chen W, Yu Z, Li Y and Liu G (2022) Influence of glacier inventories on ice thickness estimates and future glacier change projections in the Tian Shan range, Central Asia. *Journal of Glaciology*, 1–15 (doi: 10.1017/jog.2022.60)

Marshall SJ and Miller K (2020) Seasonal and interannual variability of melt-season albedo at Haig Glacier, Canadian Rocky Mountains. *Cryosphere*, **14**(10), 3249–3267 (doi: 10.5194/tc-14-3249-2020)

Marzeion B, Jarosch aH and Hofer M (2012) Past and future sea-level change from the surface mass balance of glaciers. *The Cryosphere*, **6**(6), 1295–1322 (doi: 10.5194/tc-6-1295-2012)

Marzeion B, Hock R, Anderson B, Bliss A, Champollion N, Fujita K, Huss M, Immerzeel W, Kraaijenbrink P, Malles J, Maussion F, Radić V, Rounce DR, Sakai A, Shannon S, Wal R and Zekollari H (2020) Partitioning the Uncertainty of Ensemble Projections of Global Glacier Mass Change. *Earth's Future*, **8**(7) (doi: 10.1029/2019ef001470)

Matthews T and Hodgkins R (2016) Interdecadal variability of degree-day factors on Vestari Hagafellsjökull (Langjökull, Iceland) and the importance of threshold air temperatures. *Journal of Glaciology*, **62**(232), 310–322 (doi: 10.1017/jog.2016.21)

Maussion F, Butenko A, Champollion N, Dusch M, Eis J, Fourteau K, Gregor P, Jarosch AH, Landmann J, Oesterle F, Recinos B, Rothenpieler T, Vlug A, Wild CT and Marzeion B (2019) The Open Global Glacier Model (OGGM) v1.1. *Geoscientific Model Development*, **12**(3), 909–931 (doi: 10.5194/gmd-12-909-2019)

Miles E, McCarthy M, Dehecq A, Kneib M, Fugger S and Pellicciotti F (2021) Health and sustainability of glaciers in High Mountain Asia. *Nature Communications*, **12**(1), 2868 (doi: 10.1038/s41467-021-23073-4)

Mukherjee K, Menounos B, Shea J, Mortezapour M, Ednie M and Demuth MN (2022) Evaluation of surface mass-balance records using geodetic data and physically-based modelling, place and peyto glaciers, western canada. *Journal of Glaciology*, 1–18 (doi: 10.1017/jog.2022.83)

Oerlemans J (2001) *Glaciers and climate change*. CRC Press, ISBN 9789026518133

Palazzi E, Mortarini L, Terzago S and von Hardenberg J (2019) Elevation-dependent warming in global climate model simulations at high spatial resolution. *Climate Dynamics*, **52**(5-6), 2685–2702 (doi: 10.1007/s00382-018-4287-z)

Pepin N, Bradley RS, Diaz HF, Baraer M, Caceres EB, Forsythe N, Fowler H, Greenwood G, Hashmi MZ, Liu XD, Miller JR, Ning L, Ohmura A, Palazzi E, Rangwala I, Schöner W, Severskiy I, Shahgedanova M, Wang MB, Williamson SN and Yang DQ (2015) Elevation-dependent warming in mountain regions of the world. *Nature Climate Change*, **5**(5), 424–430 (doi: 10.1038/nclimate2563)

Pfeffer WT, Arendt Aa, Bliss A, Bolch T, Cogley JG, Gardner AS, Hagen JO, Hock R, Kaser G, Kienholz C, Miles ES, Moholdt G, Mölg N, Paul F, Radić V, Rastner P, Raup BH, Rich J and Sharp MJ (2014) The Randolph Glacier Inventory: a globally complete inventory of glaciers. *Journal of Glaciology*, **60**(221), 537–552 (doi: 10.3189/2014JoG13J176)

Pramanik A, Van Pelt W, Kohler J and Schuler TV (2018) Simulating climatic mass balance, seasonal snow development and associated freshwater runoff in the Kongsfjord basin, Svalbard (1980–2016). *Journal of Glaciology*, **64**(248), 943–956 (doi: 10.1017/jog.2018.80)

Radić V, Bliss A, Beedlow aC, Hock R, Miles E and Cogley JG (2014) Regional and global projections of twenty-first century glacier mass changes in response to climate scenarios from global climate models. *Climate Dynamics*, **42**(1-2), 37–58 (doi: 10.1007/s00382-013-1719-7)

Réveillet M, Vincent C, Six D and Rabatel A (2017) Which empirical model is best suited to simulate glacier mass balances? *Journal of Glaciology*, **63**(237), 39–54 (doi: 10.1017/jog.2016.110)

Rounce DR, Hock R and Shean DE (2020a) Glacier Mass Change in High Mountain Asia Through 2100 using the Open-Source Python Glacier Evolution Model (PyGEM). *Frontiers in Earth Science*, **7** (doi: 10.3389/feart.2019.00331)

Rounce DR, Khurana T, Short MB, Hock R, Shean DE and Brinkerhoff DJ (2020b) Quantifying parameter uncertainty in a large-scale glacier evolution model using Bayesian inference: application to High Mountain Asia. *Journal of Glaciology*, **66**(256), 175–187 (doi: 10.1017/jog.2019.91)

Rounce DR, Hock R, Maussion F, Hugonnet R, Kochtitzky W, Huss M, Berthier E, Brinkerhoff D, Compagno L, Copland L, Farinotti D, Menounos B and McNabb RW (2023) Global glacier change in the 21st century: Every increase in temperature matters. *Science*, **379**(6627), 78–83 (doi: 10.1126/science.abo1324)

Sakai A and Fujita K (2017) Contrasting glacier responses to recent climate change in high-mountain Asia. *Scientific Reports*, **7**(1), 13717 (doi: 10.1038/s41598-017-14256-5)

Screen JA (2014) Arctic amplification decreases temperature variance in northern mid-to high-latitudes. *Nature Climate Change*, **4**(7), 577–582 (doi: 10.1038/nclimate2268)

Shannon S, Smith R, Wiltshire A, Payne T, Huss M, Betts R, Caesar J, Koutroulis A, Jones D and Harrison S (2019) Global glacier volume projections under high-end climate change scenarios. *The Cryosphere*, **l**, 1–36 (doi: 10.5194/tc-2018-35)

Tamarin-Brodsky T, Hodges K, Hoskins BJ and Shepherd TG (2020) Changes in Northern Hemisphere temperature variability shaped by regional warming patterns. *Nature Geoscience*, **13**(6), 414–421 (doi: 10.1038/s41561-020-0576-3)

Tang S, Vlug A, Piao S, Li F, Wang T, Krinner G, Li LZX, Wang X, Wu G, Li Y, Zhang Y, Lian X and Yao T (2023) Regional and tele-connected impacts of the Tibetan Plateau surface darkening. *Nature Communications*, **14**(1), 32 (doi: 10.1038/s41467-022-35672-w)

Ultee L, Coats S and Mackay J (2022) Glacial runoff buffers droughts through the 21st century. *Earth System Dynamics*, **13**(2), 935–959 (doi: 10.5194/esd-13-935-2022)

Vincent C and Thibert E (in review) Brief communication: Nonlinear sensitivity of glacier-mass balance attested by temperature-index models. *The Cryosphere Discussions*, **2022**, 1–13 (doi: 10.5194/tc-2022-210)

Werder MA, Huss M, Paul F, Dehecq A and Farinotti D (2020) A bayesian ice thickness estimation model for large-scale applications. *Journal of Glaciology*, **66**(255), 137–152 (doi: 10.1017/jog.2019.93)

WGMS (2020) Fluctuations of Glaciers Database. World Glacier Monitoring Service, Zurich, Switzerland (doi: 10.5904/wgms-fog-2020-08)

Yang W, Li Y, Liu G and Chu W (2022) Timing and climatic-driven mechanisms of glacier advances in Bhutanese Himalaya during the Little Ice Age. *The Cryosphere*, **16**(9), 3739–3752 (doi: 10.5194/tc-16-3739-2022)

Zekollari H, Huss M and Farinotti D (2019) Modelling the future evolution of glaciers in the European Alps under the EURO-CORDEX RCM ensemble. *Cryosphere*, **13**(4), 1125–1146 (doi: 10.5194/tc-13-1125-2019)

Zekollari H, Huss M, Farinotti D and Lhermitte S (2022) Ice-dynamical glacier evolution modeling—a review. *Reviews of Geophysics*, **60**(2) (doi: 10.1029/2021RG000754)

A APPENDIX

A.1 Snow ageing bucket system

We differentiate between snow, various firn age stages and ice by applying a monthly ageing update. At initialisation, we assume to have ice everywhere. Then, for each month, solid precipitation that has not melted in that same month goes inside the snow bucket. When melting occurs, the youngest bucket, the snow bucket, is emptied first. If this is or gets empty, the next older bucket is emptied and so on. The ageing update of the remaining snow occurs at the end of each month. The snow amount (in $\mathrm{kg\,m^{-2}}$) that did not melt over that month is transferred to the next older bucket, which is the one-month-old bucket. The same is repeated for all other buckets. If snow has fallen six years ago and has not melted, i.e., it was transferred each month to the next older bucket, it will be finally converted to ice. There is no ice bucket, as OGGM does the MB calibration before the ice thickness inversion (at this stage, OGGM does not know how much ice lies below the surface). Thus, the mass is just removed from the buckets, and the gridpoint is treated as ice if all buckets are empty. We use six years of spinup to initialise the buckets. Note that we neglect ice dynamics in this approach. The monthly ageing update option with monthly buckets is much more computationally expensive than a yearly ageing update (implemented but not used). However, the monthly ageing update option is more realistic as the degree-day factor (i.e., depending on the surface type) varies strongly between the seasons. With this bucket system, we do now have the possibility to track for each month how much snow or firn amount (in $\mathrm{kg\,m^{-2}}$) there is for each bucket and each height-gridpoint along the flowline, i.e., we can track the snow age in the vertical column in a monthly resolution.

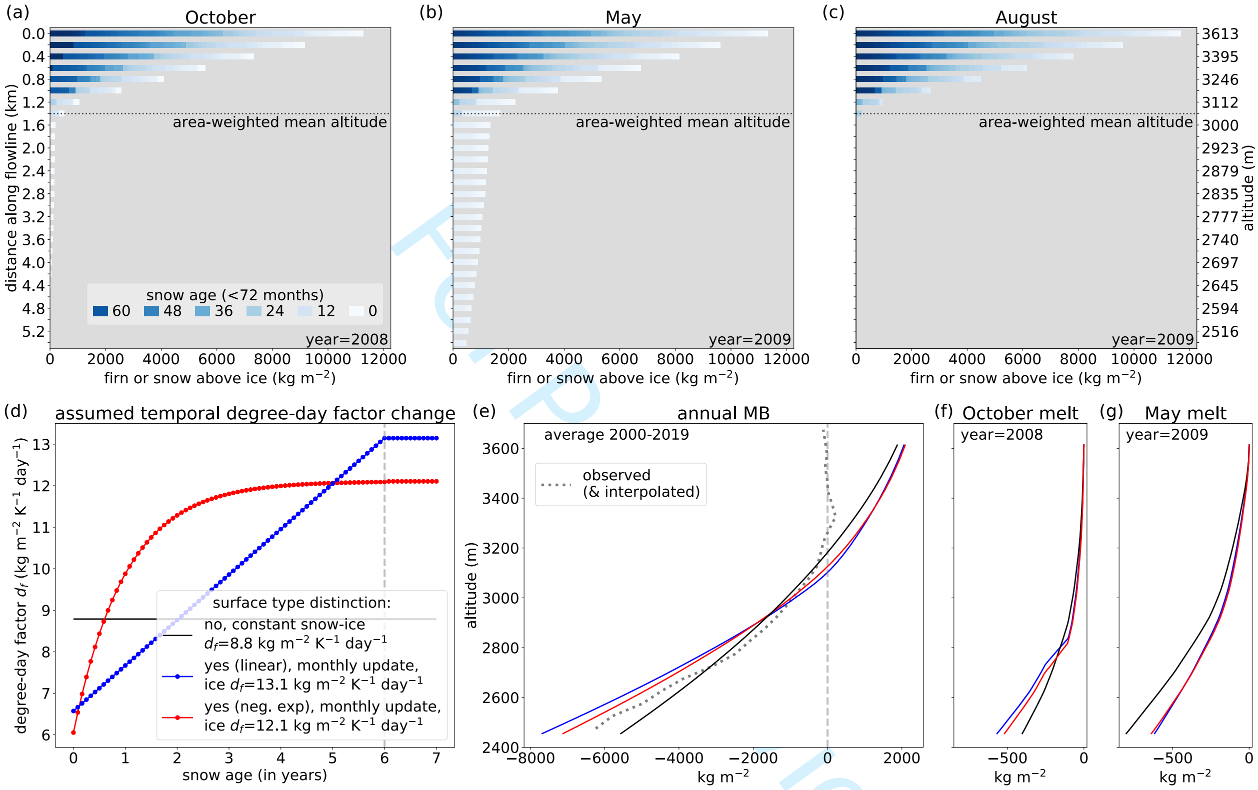

Fig. 8. Snow age tracking with snow buckets depicted for the Hintereisferner glacier for end of **(a)** October 2008, **(b)** May 2009 and **(c)** August 2009. The approximate area-weighted mean altitude of that glacier is shown. Snow is treated as ice when it is 72 months old and does not melt. In (a, b, c), the amount of ice is not shown. In **(d)**, for different assumptions of degree-day factor (d_f) change with snow age, the calibrated evolution of the snow to ice d_f is shown. In **(e)**, the resulting average altitudinal-dependent MB over 2000-2019 is shown for the different options together with the observations. In **(f, g)**, only the melt MB profile is shown for October 2008 and May 2009. With surface-type distinction, (f) more melt occurs in summer and (g) less in winter compared to no surface-type distinction due to the applied snow-to-ice gradient of d_f (specifically at lower altitudes). We show here calibration option C_5 with resulting precipitation factor (p_f)=3.45 for the temperature-index model with variable temperature lapse rates and daily climate data.

Using a monthly resolution, we can visualize the yearly cycle of surface-type distinction for a single exemplary year (here the Hintereisferner glacier in Oetztal Alps, Austria, Appendix Fig. 8). At the end of October, at the upper part of the glacier, relatively fresh snow is above the older firn layers and the actual glacier ice. In the lower part, very little fresh snow or even no snow is above the glacier (Appendix Fig. 8a). After the winter, here in May, the fresh snow is distributed equally over the glacier. However, at the lowest part, winter snow starts to melt away (Appendix Fig. 8b). In August, only ice is left on the entire lower part of the glacier, and at the upper part, winter snow and even some of the firn layers are melting away (Appendix Fig. 8c). Thus, this method is a new way to distinguish between snow, firn and ice surfaces which can be used to apply surface-type dependent degree-day factors or for potential future other applications (e.g. estimating snow densities).

Supplemental Information for

Glacier projections sensitivity to temperature-index model choices and calibration strategies

Lilian Schuster[1], David R. Rounce[2], Fabien Maussion[1]

submitted to the Annals of Glaciology

Special Issue: Ice, Snow, Water and Permafrost in a Warming World

Contents

[1]Department of Atmospheric and Cryospheric Sciences, University of Innsbruck, Innsbruck, Austria

[2]Department of Civil and Environmental Engineering, Carnegie Mellon University, Pittsburgh, PA, United States

1 Supplemental figures of the calibration and model performance

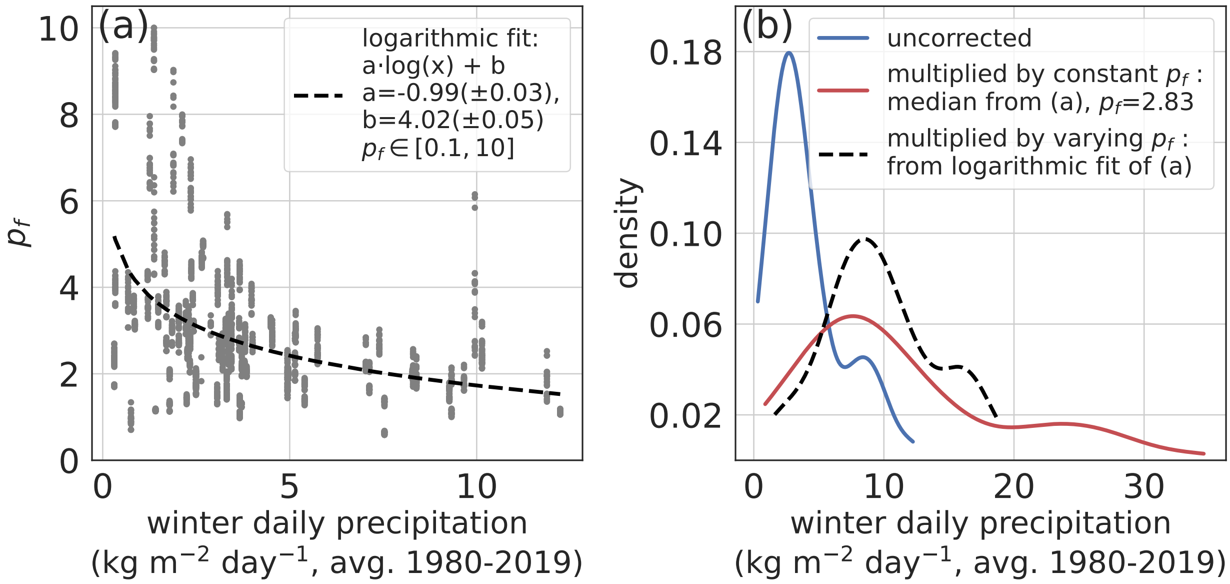

Figure S1: **(a)** Relation between winter daily precipitation and calibrated precipitation factor (p_f) for C_2 for the 114 glaciers where the calibration to match the winter MB was possible for all temperature-index model options together (correlation coefficient R^2=0.2). The logarithmic fit with one standard deviation error of the parameters is given. This relation is used to estimate glacier-specific p_f for option C_5. The only relation between calibrated p_f and glacier(-climate) characteristic that we found was with winter precipitation (i.e., average daily precipitation over the years 1980–2019 between October and April for glaciers in the Northern Hemisphere and between April and September for glaciers in the Southern Hemisphere).**(b)** Uncorrected and corrected precipitation distributions of the 114 glaciers. If the same p_f, median from (a), is applied to each glacier, the precipitation distribution width is much larger than the uncorrected one or the one using a winter precipitation dependent p_f.

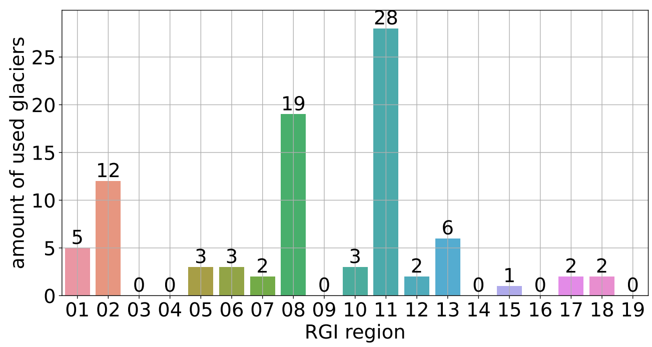

Figure S2: Amount of glaciers per RGI region that could be calibrated for all calibration and temperature-index model options (in total 88 glaciers). That means the glaciers need to have, both sufficient winter MB and annual MB measurements available as well as fitting parameter combinations for all options.

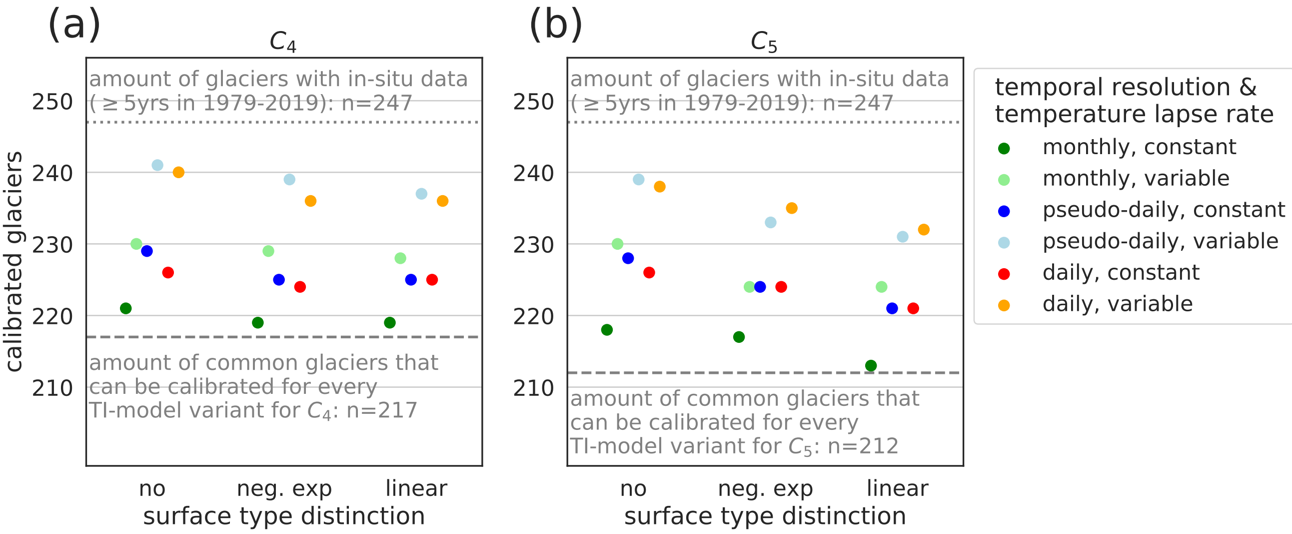

Figure S3: Amount of glaciers per temperature-index model options that could be calibrated for option **(a)** C_4 and **(b)** C_5

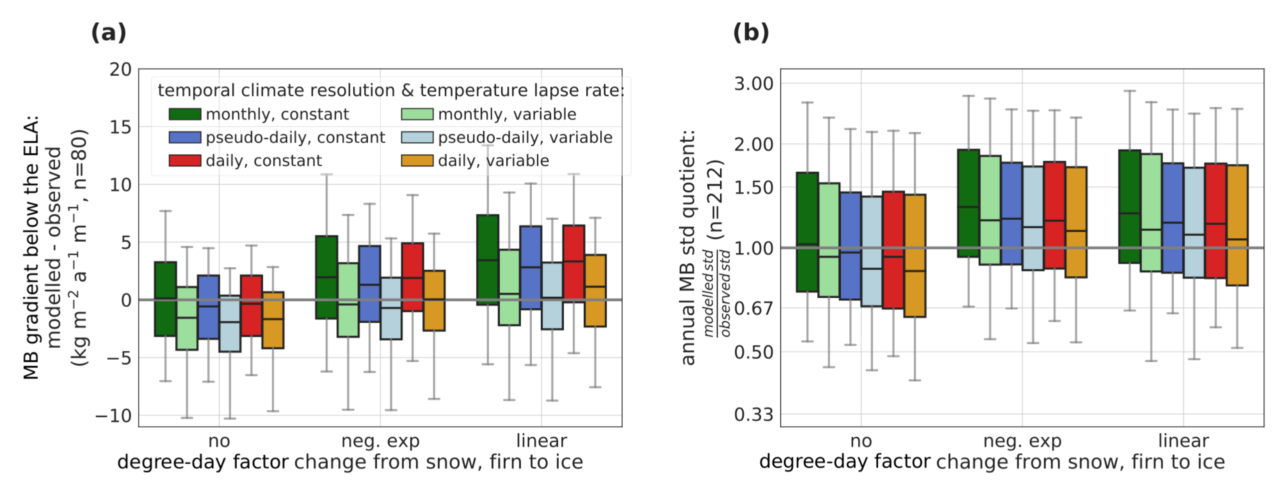

Figure S4: Temperature-index model performance for different measures from independent observations for calibration option C_5. In **(a)**, the difference between modelled and observed mean MB gradient below the equilibrium line altitude (ELA) and in **(b)** the standard deviation quotient between modelled and observed interannual MB variability are shown. The resulting distributions are represented by the $5\%_{\text{ile}}$, $25\%_{\text{ile}}$, $50\%_{\text{ile}}$ (median), $75\%_{\text{ile}}$ and the $95\%_{\text{ile}}$.

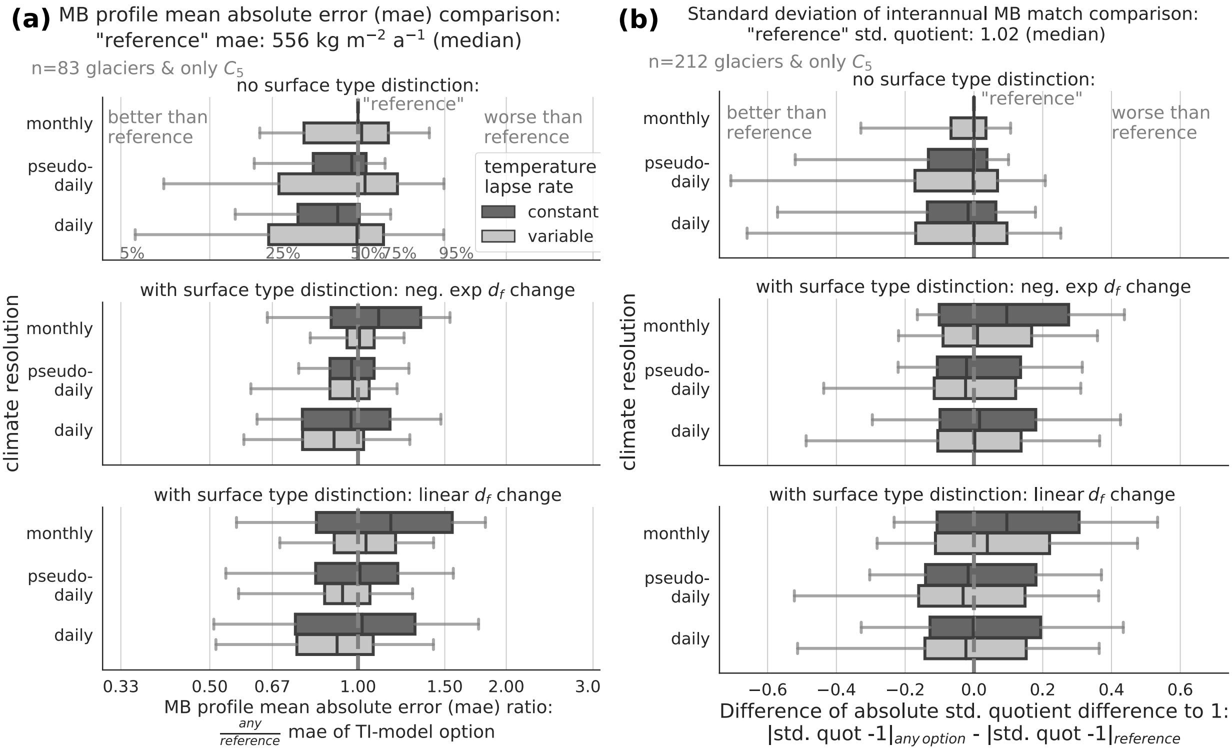

Figure S5: MB model performance comparison for different measures from independent observations for calibration option C_5. The median measure from the reference model is given and then compared to the other model options. In **(a)**, the ratio of MB profile mean absolute errors (mae) between observed and modelled mean MB profile over the observation years is shown for 83 glaciers. As we do not want to set too much weight on the wider snow or firn-covered accumulation area where uncertainties are larger, we compute the mae of the altitudinal bands without weighting for the glacier width. To compare the performance between different temperature-index model options, we divide the mae of every option through the reference model option. In **(b)**, differences in the absolute std. quotients to one (i.e., a measure of how well the interannual MB is matched) are shown for 212 glaciers. d_f stands for degree-day factor. The resulting distributions are represented by the $5\%_{\text{ile}}$, $25\%_{\text{ile}}$, $50\%_{\text{ile}}$ (median), $75\%_{\text{ile}}$ and the $95\%_{\text{ile}}$. A distribution shift to the right means, for each measure, that this option matches the validation measure worse than the reference option. The differences in the mean MB gradient absolute bias below the equilibrium line altitude are shown in Fig. 3a.

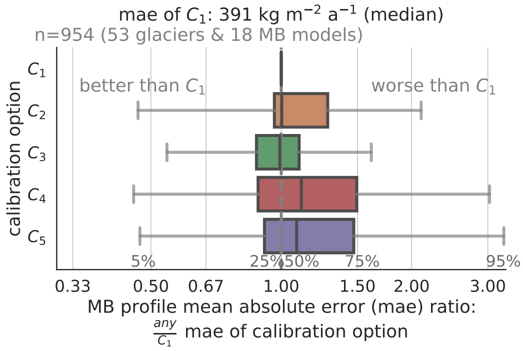

Figure S6: Same as Fig. 3b but looking into the MB profile mean absolute error (mae) ratio

2 Supplemental figures of volume projections

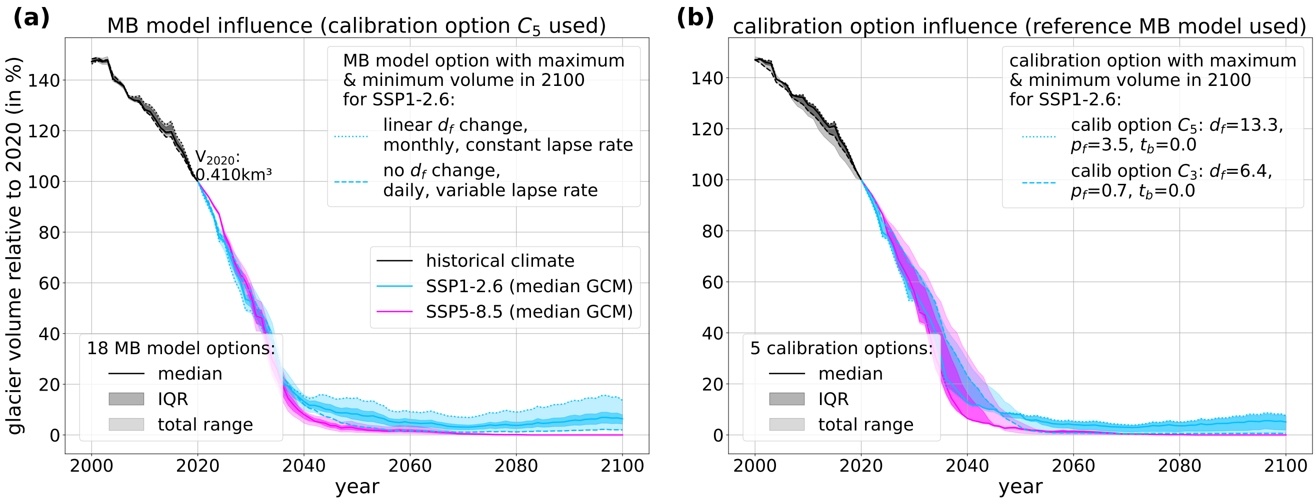

Figure S7: Same as Fig. 5, for RGI60-11.00897, i.e., Hintereisferner glacier volume projections (2000-2100) for two SSP scenarios. The interquartile range (75%ile–25%ile, IQR) and the total range resulting from **(a)** the temperature-index model options and **(b)** the calibration options are shown. d_f stands for degree-day factor, p_f for precipitation factor, and t_b for temperature bias. The volume estimates correspond to the median volume from the five GCMs.

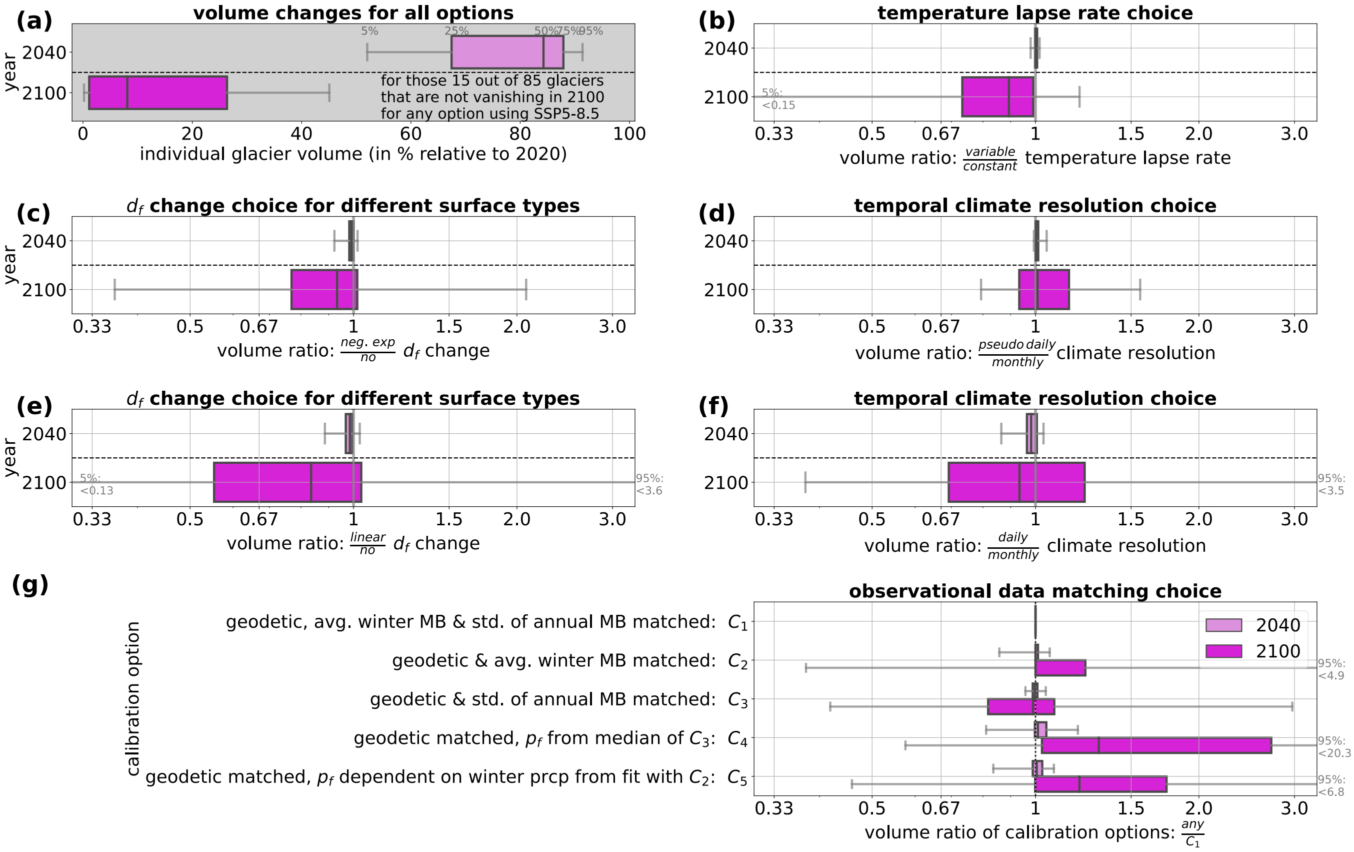

Figure S8: Similar to Fig. 6 but instead for SSP5-8.5: **(a)** Individual glacier volume changes in 2040 and 2100 for 15 glaciers that could be calibrated on all options and still exist in 2100 under the SSP5-8.5 scenario. Individual glacier volume ratios for **(b-f)** temperature-index model and **(g)** calibration options. The resulting distributions are represented by the $5\%_{\rm ile}$, $25\%_{\rm ile}$, $50\%_{\rm ile}$ (median), $75\%_{\rm ile}$ and the $95\%_{\rm ile}$. A distribution shift to the right (left) means that including this option instead of the reference option results in a larger (smaller) glacier volume than the MB model combinations that use the respective reference option. Note that the volume changes and ratios are estimated from all MB model and calibration options, i.e., (a) represents 15 glaciers $\cdot$ 5 calibration $\cdot$ $(3 \cdot 3 \cdot 2)$ temperature-index models options. Volume ratios are in total represented respectively by (b) $15 \cdot 5 \cdot (3 \cdot 3)$, in (c–f) $15 \cdot 5 \cdot (3 \cdot 2)$, and in (g) $15 \cdot (3 \cdot 3 \cdot 2)$ glaciers and options. We only look at the median volume estimates of the five GCMs.

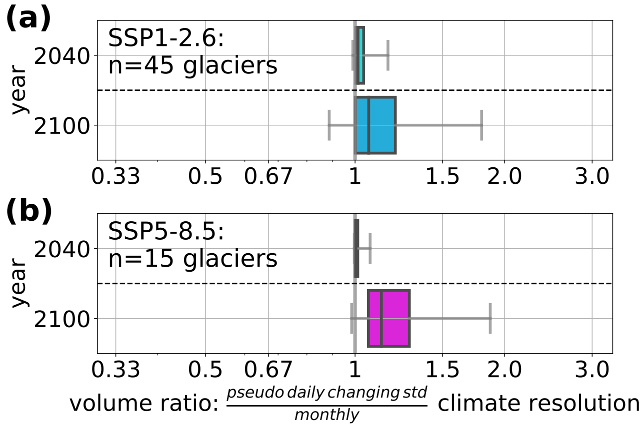

Figure S9: Additional subplot of **(a)** Fig. 6 and **(b)** Fig. S8 by comparing volume projections of another temporal climate resolution variant. "pseudo-daily changing std" is an option where the applied daily temperature standard deviation is derived from the actual daily W5E5 and future GCMs instead of using a seasonally different but interannually constant standard deviation as used in the MB model option "pseudo-daily". The resulting distributions are represented by the 5%ile, 25%ile, 50%ile (median), 75%ile and the 95%ile. In 2100, using the "pseudo-daily changing std" compared to the monthly option results in a larger projected glacier volume for more than 75% of the glaciers.

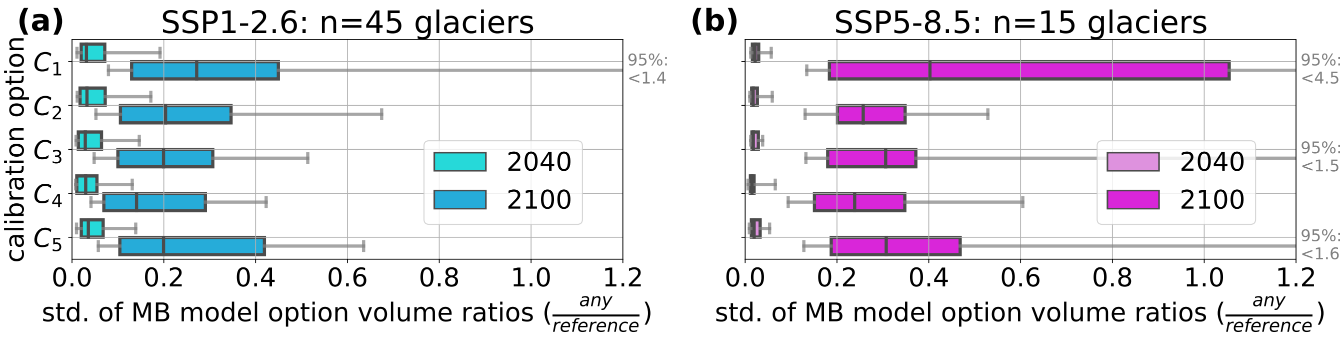

Figure S10: Standard deviation of temperature-index model option volume ratios for any vs the reference MB model option for the different calibration options (see Table 2) in the year 2040 and 2100. In **(a)**, the distribution from the common running and still in 2100 existing glaciers for SSP1-2.6 and **(b)**, respectively, for SSP5-8.5 are shown. The distribution of the standard deviation of the temperature-index model type volume ratios (for each glacier one std) is used here to compare how much the temperature-index model types vary for each calibration option.

3 Supplemental figures of runoff projections

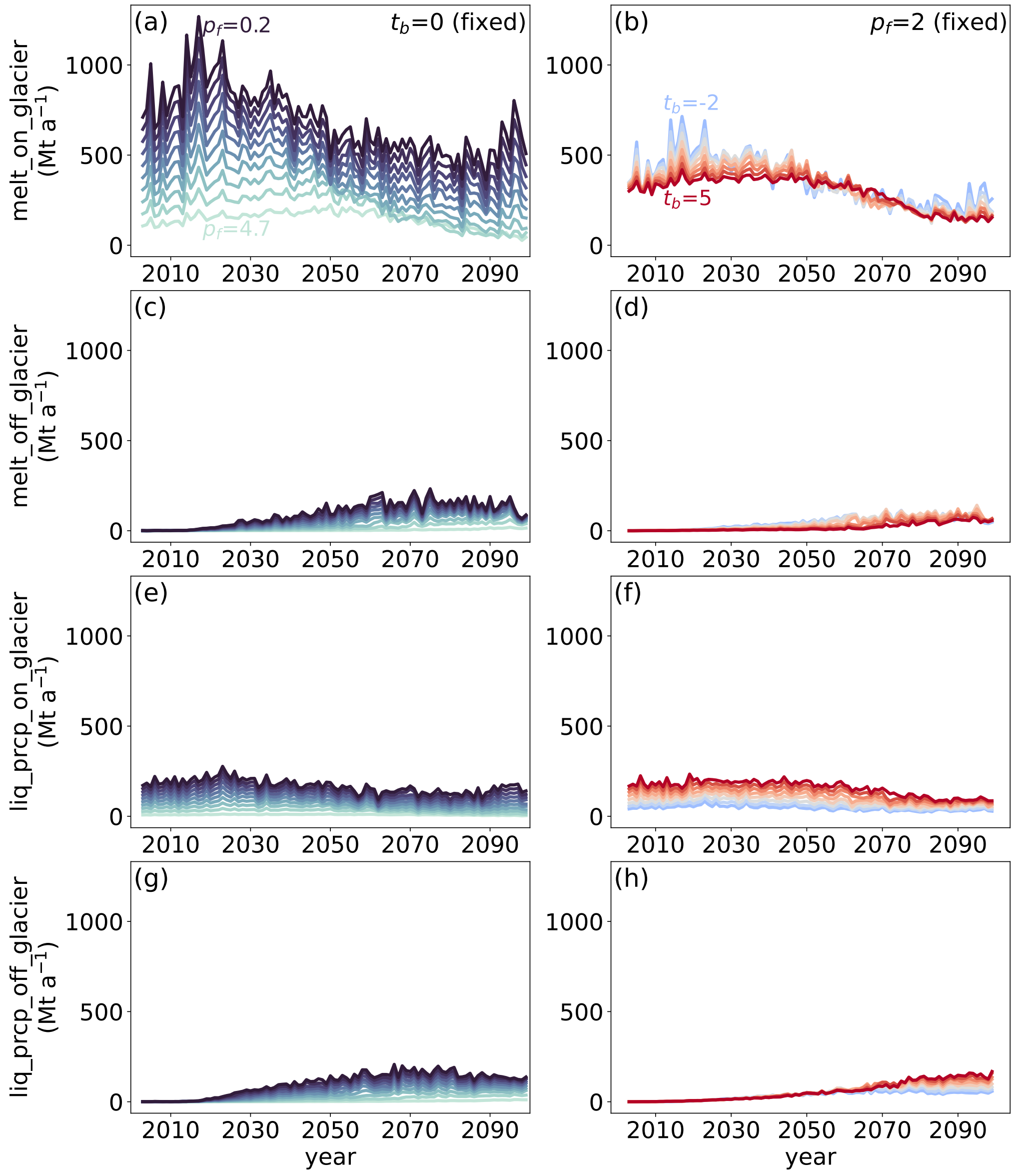

Figure S11: Additional subplots of Fig. 7 to show the influence of downscaling model parameter choice on the four different runoff components in OGGM (again for the Aletsch glacier): **(a, b)** melt on glacier, **(c, d)** melt off glacier, **(e, g)** liquid precipitation on glacier and **(g, h)** liquid precipitation off glacier. The "off"-glacier parts are coming from the former glacier area at the RGI data. Thus, the "on"-glacier components are dominant over the first decades while the "off"-glacier influence increases as the glacier melts away.

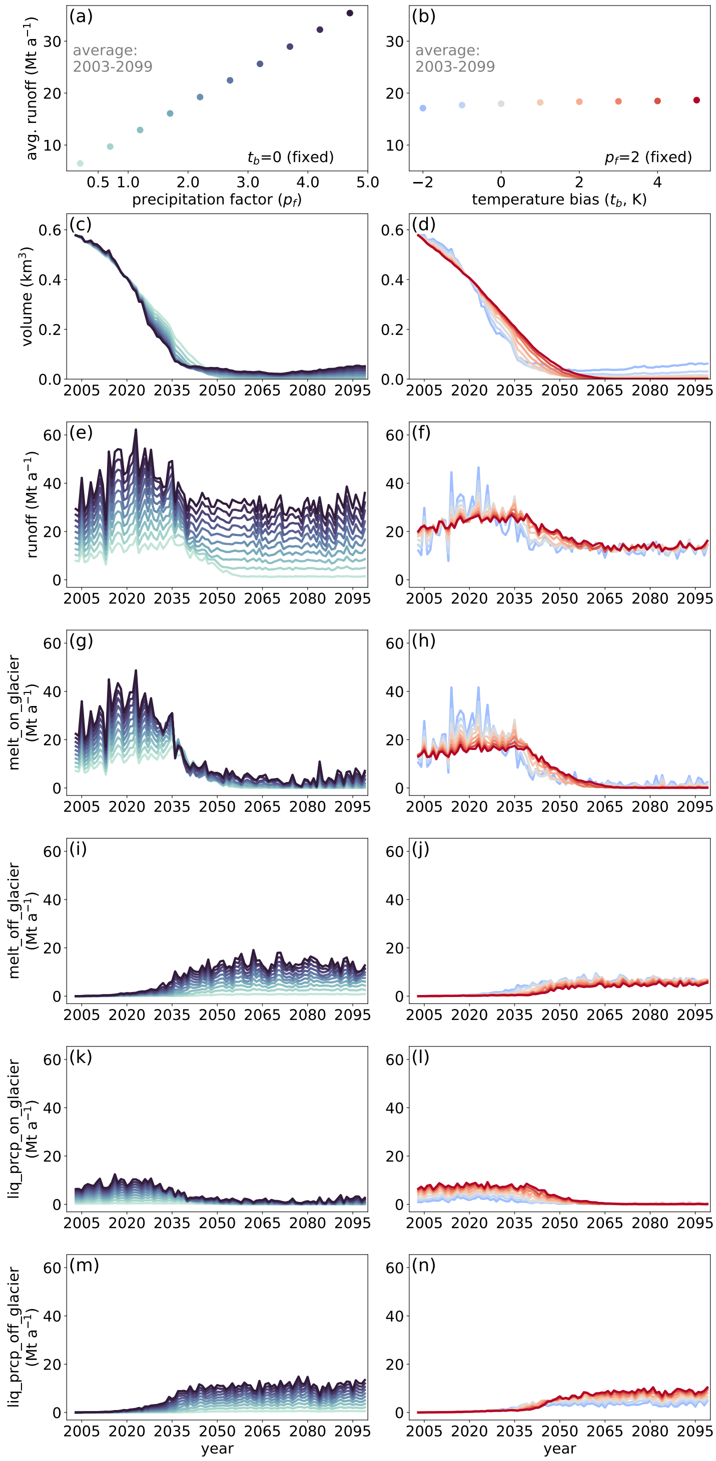

Figure S12: The equivalent Fig. 1 for runoff and volume: Influence of downscaling MB model parameters on the **(a, b)** average annual runoff, **(c, d)**, projected volume, **(e, f)** interannual runoff variability, and the four different runoff components **(g, h)** melt on glacier, **(i, j)** melt off glacier, **(k, l)** liquid precipitation on glacier and **(k, l)** liquid precipitation off glacier. It is shown here for the Hintereisferner glacier, Ötztal Alps, Austria using the reference temperature-index model during the period 2003-2099. Although all parameter combination choices match the mean specific MB equally well, they can differ substantially in volume and runoff estimates. On the left plots, **(a, c, e, g, j, k, m)**, temperature bias (t_b) is set to zero and precipitation factor (p_f) is varied while on the right plots, **(b, d, f, h, j, l, n)**, p_f is set to 2 and t_b is varied. Future projections are the median estimates from five GCMs.

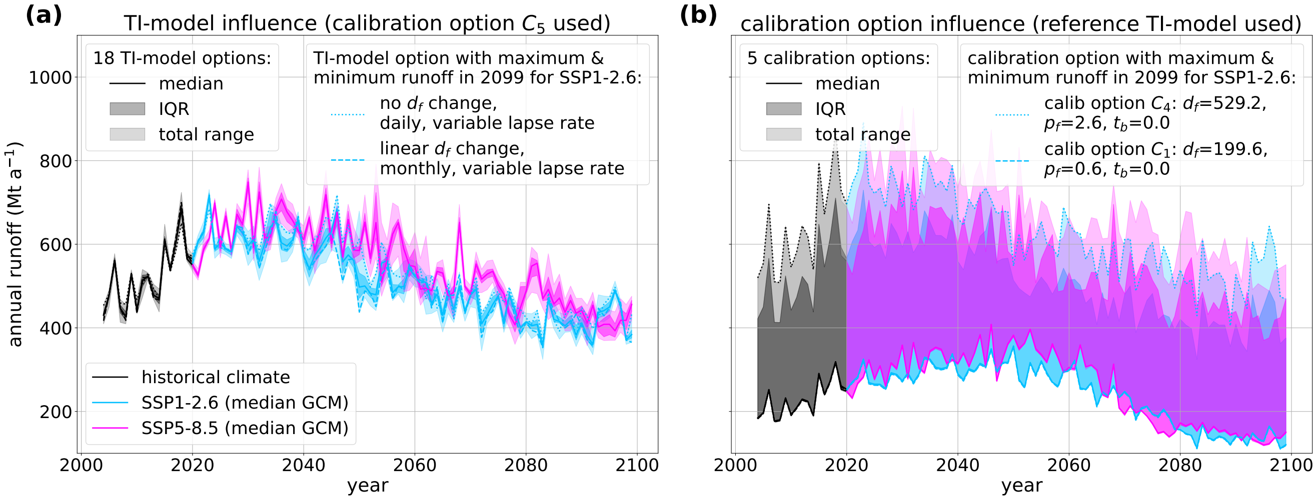

Figure S13: Aletsch glacier (RGI60-11.01450) projections for the annual runoff (same structure as in Fig. S7). Note that for this glacier, in (b), the calibrated parameters and thus projections for options C_1, C_2 and C_5 of the reference MB model are very similar. The runoff estimates correspond to the median runoff from the five GCMs.

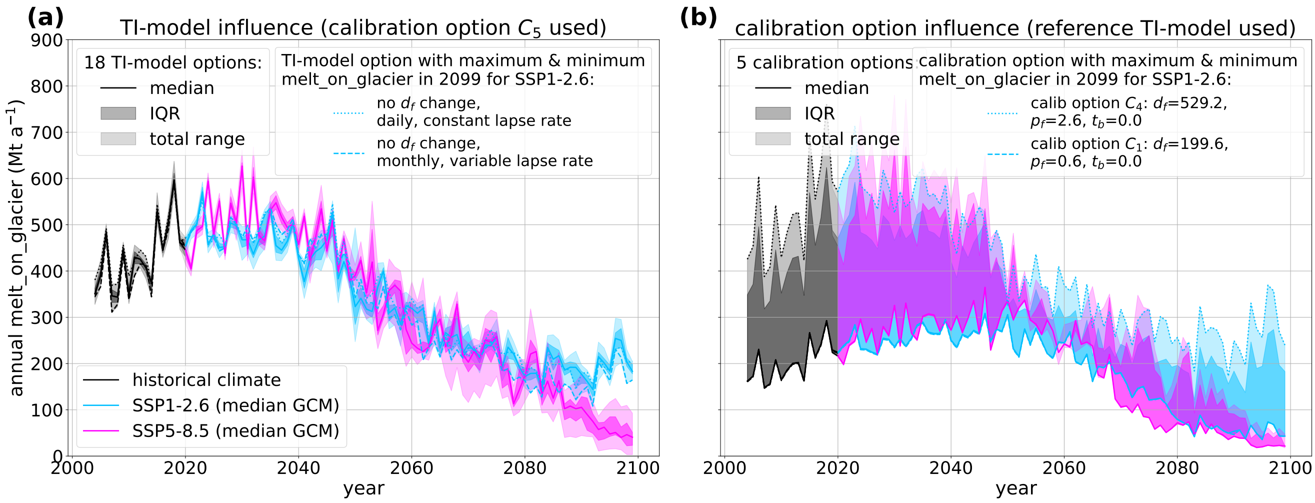

Figure S14: Aletsch glacier (RGI60-11.01450) projections for the melt on glacier contribution to the annual runoff (same structure as in Fig. S13). The melt on glacier estimates correspond to the median from the five GCMs.

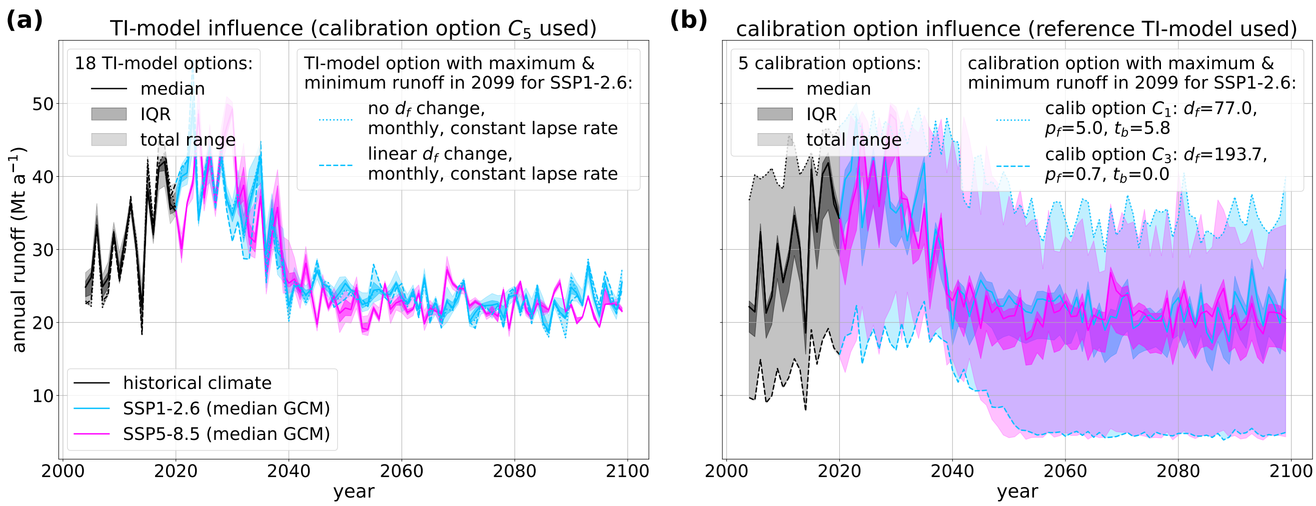

Figure S15: Hintereisferner glacier (RGI60-11.00897) projections for the annual runoff (same structure as in Fig. S7). The runoff estimates correspond to the median from the five GCMs.

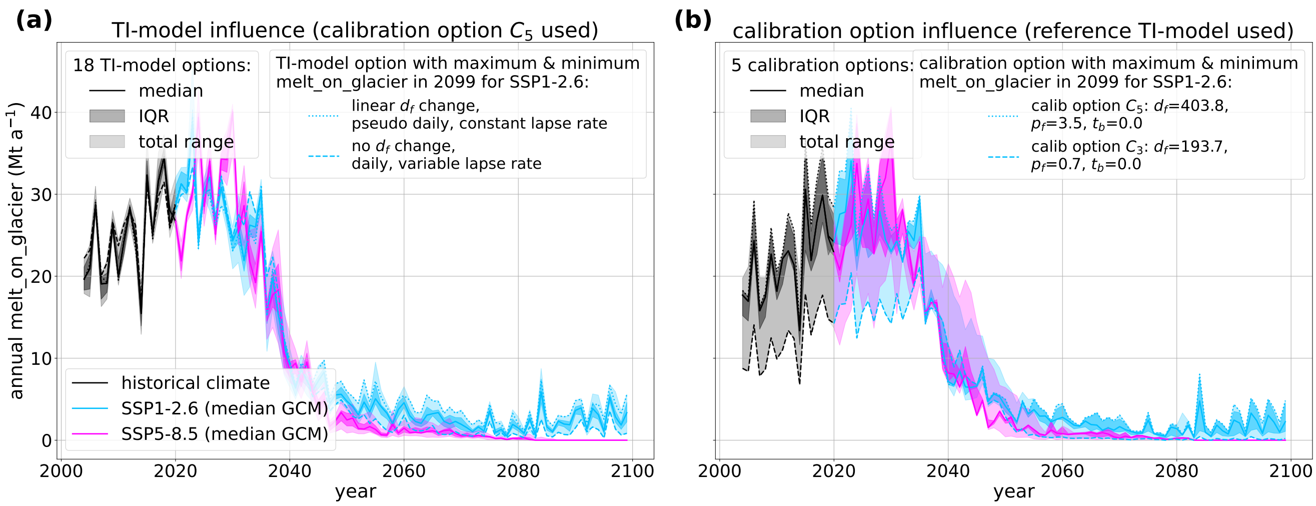

Figure S16: Hintereisferner glacier (RGI60-11.00897) projections for the melt on glacier contribution to the annual runoff (same structure as in Fig. S7). The melt on glacier estimates correspond to the median from the five GCMs.

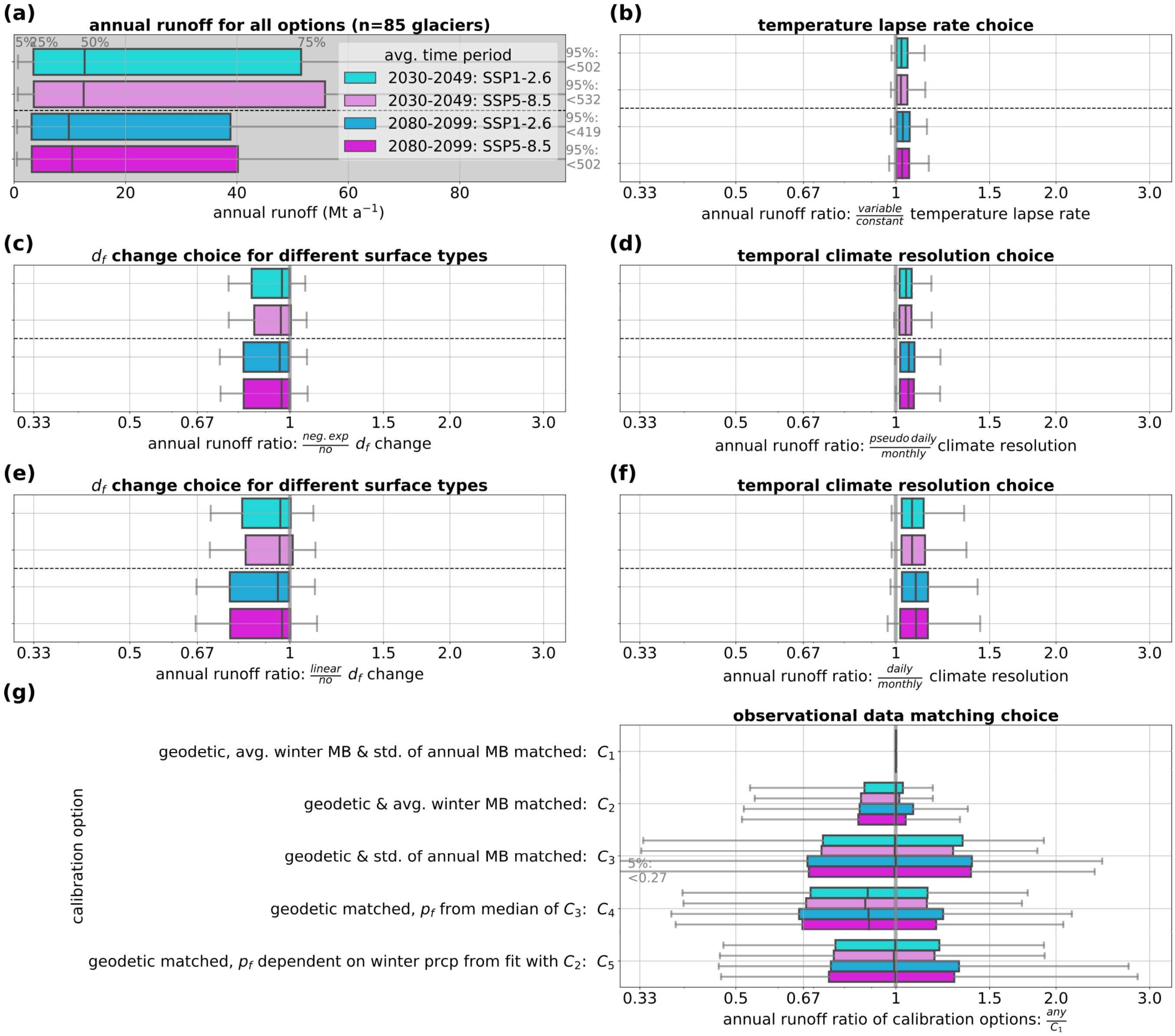

Figure S17: Glacier runoff projections for SSP1-2.6 and SSP5-8.5 for 83 glaciers with additional data. The figure is equally constructed as Fig. 6 and Suppl. Fig. S8, but here the runoff instead of the volume is shown. Note that around half of the glaciers do not exist any more in 2100 but the runoff of the former glacierized area is included in the fixed-gauge runoff.